PERK-mediated antioxidant response is key for pathogen persistence in ticks

Kristin L. Rosche[1], Joanna Hurtado[1,2#], Elis A. Fisk[1], Kaylee A. Vosbigian[1], Ashley L. Warren[1], Lindsay C. Sidak-Loftis[1], Sarah J. Wright[1], Elisabeth Ramirez-Zepp[1], Jason M. Park[1], Dana K. Shaw[1,2*]

[1]Department of Veterinary Microbiology and Pathology, Washington State University, Pullman, WA, USA

[2]School of Molecular Biosciences, Washington State University, Pullman, Washington, USA.

[#]Present address: Entrogen, Inc., 20950 Warner Center Ln, Ste B, Woodland Hills, CA 91367

Corresponding Author: *Dana K. Shaw; Dana.Shaw@wsu.edu

Running title: PERK antioxidant response promotes pathogen persistence in ticks

ABSTRACT

A crucial phase in the lifecycle of tick-borne pathogens is the time spent colonizing and persisting within the arthropod. Tick immunity is emerging as a key force shaping how transmissible pathogens interact with the vector. How pathogens remain in the tick despite immunological pressure remains unknown. In persistently infected *Ixodes scapularis*, we found that *Borrelia burgdorferi* (Lyme disease) and *Anaplasma phagocytophilum* (granulocytic anaplasmosis) activate a cellular stress pathway mediated by the endoplasmic reticulum receptor PERK and the central regulatory molecule, eIF2α. Disabling the PERK pathway through pharmacological inhibition and RNAi significantly decreased microbial numbers. *In vivo* RNA interference of the PERK pathway not only reduced the number of *A. phagocytophilum* and *B. burgdorferi* colonizing larvae after a bloodmeal, but also significantly reduced the number of bacteria that survive the molt. An investigation into PERK pathway-regulated targets revealed that *A. phagocytophilum* and *B. burgdorferi* induce activity of the antioxidant response regulator, Nrf2. Tick cells deficient for *nrf2* expression or PERK signaling showed accumulation of reactive oxygen and nitrogen species in addition to reduced microbial survival. Supplementation with antioxidants rescued the microbicidal phenotype caused by blocking the PERK pathway. Altogether, our study demonstrates that the *Ixodes* PERK pathway is activated by transmissible microbes and facilitates persistence in the arthropod by potentiating an Nrf2-regulated antioxidant environment.

INTRODUCTION

Ticks are prolific spreaders of pathogens that plague human and animal health including bacteria, viruses, and protozoan parasites[1–4]. A crucial phase in the tick-borne pathogen lifecycle is the time spent colonizing and persisting within the arthropod vector[5]. While many forces impact the way transmissible pathogens interface with their arthropod vectors, recent advances have demonstrated that tick immunity is an important influence shaping this interaction. Immune functions that respond to tick transmitted bacterial pathogens include cellular defenses, such as phagocytosis by hemocytes, and humoral defenses orchestrated by the IMD (Immune Deficiency) and JAK-STAT (Janus kinase-signal transducer and activator of transcription) pathways[6–17]. Notably, the tick IMD pathway is divergent from what has canonically been described in *Drosophila*. Ticks and other non-insect arthropods lack genes encoding key molecules such as transmembrane peptidoglycan recognition proteins that initiate the IMD pathway, and the signaling molecules *IMD* and *FADD*[10,18,19]. Instead, the tick IMD pathway responds to multiple cues such as infection-derived lipids that are sensed by the receptor Croquemort[10,11,17] and to cellular stress that is caused by infection[20,21].

Recently, the unfolded protein response (UPR) has been linked to arthropod immunity[20]. The UPR is a specialized cellular response pathway that is activated when the endoplasmic reticulum (ER) is under stress[22–24]. Three ER receptors orchestrate the UPR and function to restore cellular homeostasis: ATF6 (activating transcription factor 6), PERK (PKR-like ER kinase), and IRE1α (inositol-requiring enzyme 1α). When *Ixodes scapularis* ticks are colonized by *Borrelia burgdorferi* (Lyme disease) or *Anaplasma phagocytophilum* (granulocytic anaplasmosis), the IRE1α receptor

undergoes self-phosphorylation and pairs with TRAF2 (TNF receptor associated factor 2) to activate the IMD pathway[20]. During this process, reactive oxygen species (ROS) are also potentiated. This signaling network functionally restricts the number of *Borrelia* and *Anaplasma* that colonize the tick[20]. Furthermore, the UPR-IMD pathway connection and its pathogen restricting potential is present in several arthropods against multiple types of pathogens, suggesting that this signaling network may be an ancient mode of pathogen-sensing and vector defense against infection[20].

As vector immunity continues to be explored, a fundamental question has emerged: how are tick-borne pathogens persisting in the arthropod despite immunological pressure? Herein, we report that *B. burgdorferi* and *A. phagocytophilum* trigger phosphorylation of the central regulatory molecule, eIF2α, in *I. scapularis* ticks through the ER stress receptor PERK. Knocking down the PERK-eIF2α-ATF4 pathway *in vivo* through RNAi significantly inhibited *A. phagocytophilum* and *B. burgdorferi* colonization in ticks and reduced the number of microbes persisting through the molt. Infection-induced PERK pathway activation in *Ixodes* was connected to the antioxidant transcription factor, Nrf2. Disabling Nrf2 or the PERK pathway in tick cells caused accumulation of ROS and reactive nitrogen species (RNS) that led to greater microbial killing. This microbicidal phenotype could be rescued by exogenously supplementing antioxidants, demonstrating that the PERK pathway supports microbial persistence by detoxifying ROS/RNS. Overall, we have uncovered a mechanism at the vector-pathogen interface that promotes persistence of transmissible microbes in the arthropod despite active immune assaults.

RESULTS

Cellular stress genes are transcriptionally induced in infected, unfed I. scapularis nymphs

Infectious microbes impart cellular stress on the host[25]. For this reason, we investigated whether cellular stress responses impact how microbes survive in ticks[20]. We previously observed that the IRE1α-TRAF2 axis of the *I. scapularis* UPR responds to *A. phagocytophilum* and *B. burgdorferi* and functionally restricts pathogen colonization during a larval blood meal by crosstalking with the IMD pathway and potentiating ROS (Fig 1A)[20]. How *Anaplasma* and *Borrelia* persist in the tick despite this immunological pressure is not well-understood. In this study, we analyzed the transcriptional response of *I. scapularis* nymphs that were infected but were unfed (flat) to explore how ticks respond to persistent infection. We found that, similar to results from immediately repleted ticks[20], unfed nymphs that are infected with *A. phagocytophilum* or *B. burgdorferi* showed increased expression of genes associated with IRE1α-TRAF2 signaling (Fig 1B-D). In addition, we also found increased expression of genes that are part of the PERK pathway and another cellular stress response network termed the “integrated stress response” (ISR) (Fig 1E-I).

The ISR is a highly conserved signaling network that is activated by cellular stress in eukaryotes[26,27]. Four different stress-sensing kinases initiate the ISR in mammals: GCN2 (general control nonderepressible), HRI (heme-regulated inhibitor), PKR (protein kinase double-stranded RNA-dependent), and PERK, which is also part of the UPR network[28,29]. eIF2α is the central regulatory molecule that all ISR kinases converge on, which then activates the transcription factor ATF4 (Fig 1A). ATF4 can also act as a transcriptional repressor of genes that lead to cell death[30,31]. Although the ISR

is much less studied in arthropods relative to mammals, genome analysis demonstrates that ticks encode most ISR components with the exception of a PKR ortholog[18,21]. We found that *B. burgdorferi* or *A. phagocytophilum* infection transcriptionally induced the ISR kinases (PERK, GCN2, HRI), the eIF2α regulatory molecule, and ATF4 in flat, unfed nymphs (Fig 1E-I).

ISR activation can be monitored by probing for the phosphorylation status of eIF2α[26,29]. When eIF2α amino acid sequences from human and *I. scapularis* were aligned, we observed a good amount of sequence similarity (Supplemental Figure 1A). Importantly, the activating residue that is phosphorylated by ISR kinases, Ser51, was conserved. We therefore used a commercially raised antibody specific for phosphorylated eIF2α to monitor ISR activation in tick cells. Relative to non-treated controls, ISE6 cells infected with either *A. phagocytophilum* or *B. burgdorferi* showed a band at approximately 36 kDa, correlating with the predicted molecular weight of *I. scapularis* eIF2α (Fig 1J). When tick cells were treated with a small molecular inhibitor of eIF2α phosphorylation, ISRIB (integrated stress response inhibitor)[32], the 36 kDa band was no longer present, indicating that the band observed was specific to phosphorylated eIF2α (Fig 1J). Altogether, these data show that cellular stress responses converging on eIF2α are activated by *A. phagocytophilum* and *B. burgdorferi* in ticks.

The PERK pathway promotes A. phagocytophilum growth and survival in tick cells

To determine how eIF2α-regulated stress responses impact pathogen survival in ticks, pharmacological modulators or RNAi silencing were used in *I. scapularis* cells.

ISRIB inhibits phosphorylation of eIF2α[32], thereby shutting down the ISR. In contrast, salubrinal is an eIF2α activator and promotes ISR activity[33,34]. We observed that, each pharmacological modulator had opposing effects on *A. phagocytophilum* colonization and replication. Inhibiting eIF2α with ISRIB caused a dose-dependent decline in bacteria (Fig 2A). In contrast, promoting eIF2α activation with salubrinal conferred a survival advantage (Fig 2B). We next used an RNAi-based knockdown approach targeting either ***eIF2α*** or the downstream transcription factor, *ATF4*. In agreement with pharmacological inhibition, transcriptional silencing caused a decline in *A. phagocytophilum* numbers (Fig 2C-D), indicating that eIF2α-regulated stress responses promote pathogen survival in tick cells.

We next sought to determine which upstream stress-sensing kinase is involved during infection. RNAi knockdown was used to silence the expression of *HRI*, *GCN2*, and *PERK* in tick cells. Although significant silencing was observed for each treatment (Fig 2E-F), a defect in *A. phagocytophilum* survival was only observed with *PERK* knockdown (Fig 2G). This survival defect correlated with what was observed when ***eIF2α*** and *ATF4* were silenced (Fig 2C-D) or pharmacologically inhibited by ISRIB (Fig 2A), suggesting that PERK may be the activating kinase.

Pathogen colonization and persistence in ticks is supported by PERK, eIF2α, and ATF4

To determine whether the pro-survival role of the PERK pathway observed *in vitro* had a similar impact on microbes *in vivo,* we used RNAi in *I. scapularis* larvae together with *Anaplasma* or *Borrelia*. Distinct tissue tropisms and kinetics are exhibited in ticks by the intracellular rickettsial bacterium, *A. phagocytophilum*, and the

extracellular spirochete, *B. burgdorferi*. *A. phagocytophilum* enters the midgut with a bloodmeal and rapidly traverses the midgut epithelium to colonize the salivary glands[7,35,36]. In contrast, *B. burgdorferi* remains in the midgut during the molt and colonizes the tick between the midgut epithelium and peritrophic membrane[37,38]. Owing to these differences, we evaluated how *Ixodes* PERK signaling impacts colonization and persistence of both pathogens. An overnight siRNA immersion protocol[20] was used to silence *PERK, eIF2α,* or *ATF4* in *I. scapularis* larvae. The next day, larvae were dried and rested before being placed on infected mice. With this approach, we observed significant knockdown of targeted genes (Fig 3A, E, I; 4A, E, I).

After ticks fed to repletion, pathogen numbers were quantified at three different time points that correspond to: 1) pathogen acquisition (immediately after repletion), 2) population expansion in the tick (7-14 days, post-repletion[39]), and 3) pathogen persistence through the molt (4-6 weeks, post-repletion). Ticks evaluated immediately after repletion (Fig 3B, F, J) and 7 days post-repletion (Fig 3C, G, K) showed a 2-6X reduction in *Anaplasma* numbers, indicating that the PERK-eIF2α-ATF4 pathway has a pro-survival role *in vivo*. However, ticks silenced for *PERK* or *ATF4* as larvae did not show statistically significant differences in *Anaplasma* burden as nymphs (Fig 3D, L). This may be due to the loss of transcriptional knockdown over the duration of the molt (4-6 weeks) or pathogen numbers rebounding after escaping the midgut to the salivary glands. For *Borrelia*, knocking down *PERK*, *eIF2α*, and *ATF4* (Fig 4A, E, I) also caused a 2-10X decrease in bacterial numbers at early colonization time points (Fig 4B-C, F-G, J-K). However, in contrast to *Anaplasma*, *Borrelia* remained significantly decreased after replete larvae molted to nymphs (Fig 4D, H, L). It is not clear why *Borrelia*

198 remained restricted after the molt while *Anaplasma* did not. One possible explanation is
199 the fundamental difference in tick colonization sites, as the midgut is generally a more
200 hostile environment for invading microbes than the salivary glands[40,41]. Taken as a
201 whole, these data indicate that the *Ixodes* PERK pathway supports both extracellular
202 and intracellular tick-borne microbes *in vivo*.
203
204 *A. phagocytophilum and B. burgdorferi trigger an Nrf2 antioxidant response in ticks*
205 The microbe-supporting activity of the PERK-eIF2α-ATF4 pathway led us to ask
206 what downstream signaling events occur that functionally promote pathogen survival.
207 Genetic manipulation techniques in *I. scapularis* ticks and tick cell lines remain
208 challenging. To circumvent this limitation, we employed a surrogate reporter system to
209 interrogate downstream signaling events from the PERK pathway. A collection of
210 luciferase reporter plasmids with promoter sequences for transcription factors
211 associated with ER stress (XBP1, NF-κB, CHOP, SREBP1, and Nrf2) were transfected
212 into HEK293 T cells. Transfected cells were then either infected with *A.*
213 *phagocytophilum* or *B. burgdorferi* or left uninfected. After 24 hrs, luciferase activity was
214 quantified to ascertain the transcriptional activity of each promoter (Fig 5A-B). In
215 agreement with previous reports[20], XBP1 activation was not observed with either *A.*
216 *phagocytophilum* or *B. burgdorferi.* In contrast, the immunoregulatory transcription
217 factor NF-κB was significantly induced by both, which is also in agreement with previous
218 findings[42–45]. Infection did not induce CHOP or SREBP1 activity, but did robustly
219 activate the antioxidant regulator Nrf2 (nuclear factor erythroid 2–related factor 2) (Fig
220 5A-B).

Nrf2 is an evolutionarily conserved cap'n'collar transcription factor that coordinates antioxidant responses[46–50]. It functions by binding to a consensus DNA sequence (antioxidant response elements (ARE)) in the promoter regions of Nrf2-regulated genes[51,52]. To identify an Nrf2 ortholog in *I. scapularis*, we used the human Nrf2 protein sequence to query the tick genome[53]. A BLAST analysis returned the *Ixodes* protein XP_042149334.1. Although *I. scapularis* Nrf2 had low sequence conservation with human Nrf2 (Supplemental Fig 2A), it did display a high degree of structural conservation when modeled with AlphaFold (Fig 5C-D; *Ixodes* Nrf2- blue; Human Nrf2- orange; Supplemental Fig 2B). Notably, amino acids within the Basic Leucine Zipper (bZIP) domain of Nrf2 that mediate DNA interactions with promoter ARE regions[54] were well-conserved in the *Ixodes* protein (R877, R880, R882, N885, A888, A889, R893, R895, K896; Supplemental Fig 2A; Fig 5D).

To determine if *nrf2* transcriptionally responds to infection, we evaluated *nrf2* gene expression in flat, unfed nymphs. We observed significantly higher *nrf2* expression in nymphs infected with *A. phagocytophilum* and *B. burgdorferi* relative to uninfected controls (Fig 5E). Since vertebrate Nrf2 regulates basal and inducible antioxidant genes, we next asked whether the *Ixodes* Nrf2 ortholog influences the tick cell redox environment. Tick cells were transfected with silencing RNAs against *nrf2* or with scrambled controls. Cells were then infected with *A. phagocytophilum* and reactive oxygen species (ROS) were measured with the fluorescent indicator 2′,7′-dichlorofluorescein diacetate (DCF-DA). We found that depleting *Ixodes nrf2* caused a significantly higher amount of ROS when compared to scrambled controls (Fig 5F).

ROS is a potent antimicrobial agent and it is well-established that *A. phagocytophilum* and *B. burgdorferi* are sensitive to ROS-mediated killing[55–58]. Considering Nrf2's role as an antioxidant regulator, we reasoned that silencing *nrf2* expression should enhance microbial killing owing to accumulated ROS. Accordingly, we found that when *nrf2* was knocked down in tick cells, there was a significant decline in *A. phagocytophilum* and *B. burgdorferi* survival (Fig 5G-H). Collectively, these results support the conclusion that *Ixodes* Nrf2 is induced during infection and functionally promotes an antioxidant response, which confers a pro-survival environment for transmissible microbes in the tick.

Antioxidant activity of the PERK-eIF2α-ATF4 pathway protects pathogen survival in ticks

A. phagocytophilum and *B. burgdorferi* induce Nrf2, which is a transcriptional activator downstream from the PERK pathway[27]. We therefore asked whether blocking eIF2α during infection would influence the redox environment in ticks. Tick cells were either uninfected, infected (*A. phagocytophilum* or *B. burgdorferi*), or treated with the eIF2α inhibitor ISRIB prior to infection. Kinetic measurements of ROS and RNS were monitored in tick cells with the fluorescent reporters DCF-DA (ROS) or 4,5-diaminoflurescein diacetate (RNS) (Fig 6A-D). In untreated cells, *A. phagocytophilum* infection caused a rise in ROS that peaked at 24 hrs. Thereafter, ROS levels declined, which is consistent with reports that *A. phagocytophilum* infection suppresses ROS[59–62]. However, when eIF2α signaling is blocked with the ISRIB inhibitor, *A. phagocytophilum* caused increased ROS throughout infection that never declined (Fig 6A; Supplemental Figure 3A). Similarly, *B. burgdorferi* induced ROS in tick cells and treating with ISRIB

showed greater accumulation of ROS than infection alone (Fig 6B; Supplemental Figure 3A). Inhibiting eIF2α had similar impacts on RNS in tick cells infected with *A. phagocytophilum* and *B. burgdorferi* (Fig 6C-D; Supplemental Figure 3B). Combining ISRIB with infection conditions caused significantly higher RNS compared to infection alone. Unexpectedly, we also observed that untreated infection conditions showed a decline in RNS, which may suggest that *Anaplasma* and *Borrelia* suppress nitrosative stress in the tick. Collectively, these data indicate that eIF2α signaling functionally coordinates an antioxidant response in tick cells during infection.

We next asked if the antioxidant environment potentiated by the PERK-eIF2α-ATF4 pathway was the functional mechanism that supports pathogen survival in ticks. We first established that antioxidants enhance microbial survival in ticks. Tick cells that were supplemented with the antioxidant N-acetyl cysteine (NAC) during infection showed significantly more *A. phagocytophilum* or *B. burgdorferi* survival when compared to untreated controls (Fig 6E-F). We then asked if the antioxidant activity of NAC could rescue the microbicidal phenotype caused by silencing *perk*. Tick cells were treated with silencing RNA against *perk* or scrambled controls, then infected with *A. phagocytophilum* or *B. burgdorferi* with and without NAC. As previously observed (Fig 2G), silencing the expression of *perk* caused a significant decrease in pathogen survival. However, supplementing with exogenous antioxidants rescued the bactericidal effect caused by blocking the PERK pathway (Fig 6G-H). Altogether, our findings support a model where transmissible pathogens activate the PERK-eIF2α-ATF4 pathway, which functionally supports pathogen persistence in ticks through an Nrf2-mediated antioxidant response (Fig 7).

DISCUSSION

How pathogens persist in the tick is likely a multifaceted topic involving complex interactions orchestrated by both the microbe and the arthropod. In this article, we shed light on one aspect of this subject by demonstrating that *Anaplasma* and *Borrelia* infection activates the *Ixodes* PERK-eIF2α-ATF4 stress response pathway, which facilitates pathogen survival. The microbe-benefiting potential of this pathway was ultimately connected to an antioxidant response that is mediated by the *Ixodes* Nrf2 ortholog. Collectively, our findings have uncovered a piece of the puzzle in understanding how pathogens can persist in the tick despite immunological pressure from the arthropod vector.

A. phagocytophilum and *B. burgdorferi* have significantly different lifestyles (obligate intracellular vs. extracellular) and tissue tropisms (salivary glands vs. midgut), but both induce a state of oxidative stress upon tick colonization[20]. Given that these microbes are susceptible to killing by oxidative and nitrosative stress[55–58,62–67], it is perhaps not surprising that both would benefit from an antioxidant response in the tick. However, some discrepancy between *Anaplasma* and *Borrelia* survival phenotypes was observed at different time points *in vivo.* Bacterial colonization was decreased in larvae when *PERK*, *eIF2α*, or *ATF4* were knocked down by RNAi (Fig 3-4). In contrast, *Borrelia* remained significantly reduced in molted nymphs, but *Anaplasma* numbers rebounded. This may be attributable to differences in tissue tropisms for each pathogen. *Anaplasma* rapidly escapes the midgut and colonizes the salivary glands[7,35,36], whereas *B. burgdorferi* remains in the midgut during the molt[37,38]. The midgut is a niche that is

312 generally hostile to microbes owing to several factors including ROS and RNS
313 production[40,41,64,65] and may explain why *Borrelia* numbers are restricted even after
314 larvae molt to nymphs. The *Ixodes* salivary gland environment also produces ROS and
315 RNS[64], but antioxidant proteins found in salivary glands, such as the periredoxin
316 Salp25D[68], may protect *Anaplasma* and explain why pathogen numbers rebounded
317 after the molt.

318 Since *A. phagocytophilum* and *B. burgdorferi* are susceptible to oxidative and
319 nitrosative damage[55–58,62–67], these microbes may be inducing the *Ixodes* PERK-eIF2α-
320 ATF4-Nrf2 pathway to create a more hospitable environment and facilitate persistence.
321 *A. phagocytophilum* replicates intracellularly and secretes a suite of effectors that
322 manipulate host cell biology and promote the formation of a replicative niche. Although
323 only one tick-specific effector has been characterized to date[69], it is conceivable that
324 *Anaplasma* manipulates PERK pathway activation in the tick with secreted effector
325 molecules. *B. burgdorferi* replicates extracellularly and does not encode any secretion
326 systems for effector transport, which makes direct host-cell manipulation less-likely.
327 However, it is possible that *Borrelia* may transport small molecules[63] that could activate
328 the PERK pathway and promote an antioxidant response. Alternatively, the PERK-
329 eIF2α-ATF4-Nrf2 signaling cascade may be responding to general stress signals
330 caused by infection[70]. For example, pathogens can secrete toxic by-products, compete
331 with the host for limiting amounts of nutrients, and/or cause physical damage to host
332 cells[25]. Our previous study demonstrated that both *Borrelia* and *Anaplasma* activate the
333 IRE1α-TRAF2 branch of the UPR in ticks, which results in the accumulation of ROS[20].
334 When this pathway was inhibited, ROS levels were either partially (*Anaplasma*) or

completely (*Borrelia*) mitigated. Since oxidative stress is an important stimuli that triggers the UPR[71,72], it is possible that ROS potentiated by the IRE1α-TRAF2 pathway is the signal that activates the PERK pathway at later time points and results in an antioxidant response. From this perspective, the PERK-eIF2α-ATF4-Nrf2 pathway may be a host-driven response that promotes the preservation of "self".

Unexpectedly, we observed that *A. phagocytophilum* and *B. burgdorferi* caused a decline in RNS that began either a few hours after infection (*A.p.)* or after 2 days (*B.b.*) (Fig 6C-D). A potential explanation for this could be increased Arginase expression. Arginase competes for the nitric oxide synthase substrate L-arginine and is therefore a potent inhibitor of nitric oxide production[73]. Villar *et al* reported that *Ixodes arginase* expression levels are significantly increased in *A. phagocytophilum*-infected ticks[74], which could explain the rapid decline in RNS we observed after *Anaplasma* infection (Fig 6C). Similarly, a recent report by Sapiro *et al* analyzed *I. scapularis* nymphs by mass spectrometry and reported that Arginase was enriched with *B. burgdorferi* after 4 days of feeding, but not at early time points[75]. This may explain why RNS also decreased with *B. burgdorferi* (Fig 6D), but only after 48 hours of infection.

The Nrf2 gene regulatory network has not yet been characterized in *I. scapularis*. Mammalian Nrf2 regulates components of the glutathione and thioredoxin antioxidant systems as well as enzymes involved in NADPH regeneration[76,77]. Given that ROS levels increased in tick cells when Nrf2 was knocked down (Fig 5F), it is reasonable to speculate that similar antioxidant genes are regulated by *Ixodes* Nrf2. Moreover, it is well-established that tick-borne microbes benefit from antioxidant gene expression in the tick[68,78–85]. For example, manipulating selenium-related antioxidant gene expression

has microbicidal consequences for microbes in the tick[78–80,83,85,86]. This is in agreement with our findings that Nrf2 expression promotes *Borrelia* and *Anaplasma* survival (Fig 5G-H) and further indicates that the *Ixodes* Nrf2 coordinates an antioxidant gene network.

Between human and *Ixodes* Nrf2, we observed structural conservation in the bZIP domain with 100% conservation of the amino acids that make direct contact with DNA (Fig 5C-D). However, there was very low sequence conservation (Supplemental Fig 2A) and the *Ixodes* Nrf2 is almost 400 amino acids longer than human Nrf2. This may suggest that there are regulatory mechanisms or protein-protein interactions that are unique to the tick. In addition to protein differences, the *Ixodes* Nrf2-regulated gene network also appears to be divergent. For example, heme oxygenase is an important cytoprotective protein regulated by Nrf2 in most eukaryotes and has been implicated in disease tolerance[87]. However, chelicerates do not have a gene encoding heme oxygenase[88]. Altogether, this suggests that there are differences in Nrf2 and the genes it coordinates between ticks and other eukaryotes, which may be tailored to the life histories of each organism. The extent of divergence between *Ixodes* Nrf2 and other eukaryotes is a question that remains unanswered at this time.

Collectively, our findings illustrate a scenario where early tick infection triggers IREα-TRAF2 signaling leading to IMD pathway activation and ROS production[20], while persistent infection induces the PERK pathway and an antioxidant response through Nrf2 that supports pathogen survival (Fig 7). Innate immune mediators, such as AMPs and ROS, have potent antimicrobial activity but the non-specificity of these molecules can also cause damage to host tissues[70]. We speculate that the PERK-driven

antioxidant response in persistently infected ticks is a host-driven response aimed at reducing collateral damage to "self". Ultimately this network preserves tick fitness, but also promotes pathogen persistence. The result is a balance between microbial restriction and host preservation that promotes arthropod tolerance to infection by transmissible pathogens.

METHODS

Bacteria and animal models

Roswell Park Memorial Institute (RPMI) 1640 medium supplemented with 10% heat-inactivated fetal bovine serum (FBS; Atlanta Biologicals, S11550) and 1x Glutamax (Gibco, 35050061) was used to culture *A. phagocytophilum* strain HZ in HL60 cells (ATTC, CCL-240). Cultures were maintained between 1 x 10^5-1 x 10^6 cells/ml at 37°C in the presence of 5% CO_2. Mice were infected with 1 x 10^7 host cell free *A. phagocytophilum* in 100µl of PBS (Intermountain Life Sciences, BSS-PBS) intraperitoneally as previously described[20,89]. Six days post-infection 25-50µl of infected blood was collected from the lateral saphenous vein of each mouse and *A. phagocytophilum* burdens assessed via quantitative PCR (*16s* relative to mouse *β-actin*[20,90,91]).

B. burgdorferi B31 (MSK5[20,92]) was grown at 37°C with 5% CO_2 in modified Barbour-Stoenner-Kelly II (BSK-II) medium supplemented with 6% normal rabbit serum (NRS; Pel-Freez, 31126-5). Density and growth phase of the spirochetes were assessed by dark-field microscopy. Prior to infection, plasmid verification was performed as previously described[20,92]. Mice were inoculated with 1 x 10^5 low passage

spirochetes in 100µl of 1:1 PBS:NRS intradermally. Mice were bled from the lateral saphenous vein at 7d post-infection. 25-50µl of *B. burgdorferi*-infected blood was cultured in BSK-II medium and examined for the presence of spirochetes by dark-field microscopy[20,93,94].

Male C57BL/6 mice, aged 6-10 weeks old, obtained from colonies maintained at Washington State University were used for all experiments. Guidelines and protocols approved by the American Association for Accreditation of Laboratory Animal Care (AAALAC) and by the Office of Campus Veterinarian at Washington State University (Animal Welfare Assurance A3485-01) were used for all experiments utilizing mice. The animals were housed and maintained in an AAALAC-accredited facility at Washington State University in Pullman, WA. All procedures were approved by the Washington State University Biosafety and Animal Care and Use Committees.

Ixodes scapularis ticks at the larval stage were obtained from the Biodefense and Emerging Infectious Diseases (BEI) Research Resources Repository from the National Institute of Allergy and Infectious Diseases (www.beiresources.org) at the National Institutes of Health or from Oklahoma State University (OSU; Stillwater, OK, USA). Ticks were maintained in a 23°C incubator with 16:8h light:dark photoperiods and 95-100% relative humidity.

Tick cell and HEK293 T cultures

I. scapularis embryonic cell lines ISE6 and IDE12 were cultured at 32°C with 1% CO_2 in L15C-300 and L15C media, respectively. These growth media were supplemented with 10% heat-inactivated FBS (Sigma, F0926), 10% tryptose phosphate

broth (TBP; BD, B260300), and 0.1% lipoprotein bovine cholesterol (LPBC; MP Biomedicals, 219147680)[20,95].

HEK293 T cells were maintained in Dulbecco's modified Eagle medium (DMEM; Sigma, D6429) supplemented with 10% heat-inactivated FBS (Atlanta Biologicals; S11550) and 1x Glutamax. Cells were maintained in T75 culture flasks (Corning; 353136) at 33°C or 37°C in 5% CO_2.

Pharmacological treatments and RNAi silencing

ISE6 and IDE12 cells were seeded at 1 x 10^6 cells per well in a 24-well plate and pretreated with ISRIB (Cayman Chemical, 16258), or salubrinal (Thermo Scientific, AAJ64192LB0) for 1h prior to infection. Cells were infected with *A. phagocytophilum* or *B. burgdorferi* at an MOI of 50 for 18h alone or in the presence of 50mM N-acetyl cysteine (NAC; Sigma, A7250). Cells were collected in RIPA buffer (for immunoblotting) or TRIzol for RNA (Invitrogen, 15596026). RNA was extracted with the Direct-zol RNA Microprep Kit (Zymo; R2062) and cDNA was synthesized from 300-500ng total RNA using the Verso cDNA Synthesis Kit (Thermo Fisher Scientific, AB1453B). Bacterial burden was assessed by qRT-PCR with iTaq universal SYBR Green Supermix (Bio-Rad, 1725125). Cycling conditions used were as recommended by the manufacturer.

Transfection experiments used siRNAs and scrambled controls (scRNAs) synthesized with the Silencer siRNA Construction Kit (Invitrogen, AM1620). ISE6 or IDE12 cells were seeded 1 x 10^6 cells per well in a 24-well plate or 2.5 x 10^5 per well in a 96-well plate. 3µg of siRNA or scRNA in conjunction with 2.5µl Lipofectamine 2000 (Invitrogen, 11668027) were transfected into tick cells overnight in 24-well plates. 1µg of

siRNA or scRNA with 1µl Lipofectamine 2000 was used for 96-well plates. Cells were infected with *A. phagocytophilum* (MOI 50) or *B. burgdorferi* (MOI 50) for 18h. Cells infected with *Anaplasma* had the cell culture supernatant removed before collecting in TRIzol. Cells infected with *Borrelia* had both cells and supernatant collected in TRIzol. RNA was isolated and transcripts assessed by qRT-PCR as described above. All data are expressed as means ± SEM.

Polyacrylamide gel electrophoresis and immunoblotting

Protein concentrations from cells collected in RIPA buffer were quantified by bicinchoninic acid (BCA) assay (Pierce; 23225). 25µg of protein was loaded onto a 4-15% MP TGX precast cassette (Bio-Rad; 4561083) and proteins were separated at 100V for 1 h 25 min. Proteins were transferred to a polyvinylidene difluoride (PVDF) membrane and were blocked with 5% BSA (bovine serum albumin) in TBS-T (1x tris-buffered saline containing 0.1% Tween 20) for 1 to 2 h at room temperature. The eIF2α antibody (1:500; EMD Millipore 07-760-I) was incubated with the PVDF membrane overnight at 4°C in 5% BSA in TBS-T. The following day a secondary antibody was applied (donkey anti-rabbit–HRP; Thermo Fisher Scientific; A16023; 1:2,000). Blots were visualized with enhanced chemiluminescence (ECL) Western blotting substrate (Thermo Fisher Scientific; 32106).

ROS and RNS assays

1.68 x 10^5 ISE6 cells per well were seeded in a 96-well plate with black walls and clear bottoms (Thermo Scientific, 165305). All wells were treated with the fluorescent detection probes 2',7'-dichlorofluorescein diacetate (10µM, DCF-DA; Sigma, D2926) or

4,5-diaminoflurescein diacetate (5µM, DAF-2DA; Cayman Chemical, 85165) for 1h in Ringer Buffer (155mM NaCl, 5mM KCl, 1mM $MgCl_2 \cdot 6H_2O$, 2mM $NaH_2PO_4 \cdot H_2O$, 10mM HEPES, and 10mM glucose) [20,96]. Cells were treated with the probe alone or in the presence of 1µM ISRIB. Buffer was removed and cells washed with room temperature PBS. *A. phagocytophilum* or *B. burgdorferi* were then added at an MOI of 50 in the presence of ISRIB or vehicle control (DMSO). Fluorescence was measured at 504nm/529nm at the indicated times and data are graphed as fold change of relative fluorescence units (RFU) normalized to the negative control ± SEM.

Luciferase reporter assay

HEK293 T cells were seeded in white-walled, clear-bottom 96-well plates (Greiner Bio-One, 655098) at a density of 1 x 10^4 cells per well. The following day, cells were transfected with 0.05µg of each vector from the UPR/ER stress response luciferase reporter vector set (Signosis, LR-3007) and 0.5µl of Lipofectamine 2000 in Opti-MEM I reduced-serum medium (Gibco, 31985062). Transfections were allowed to proceed overnight. The following day, the medium containing the plasmid-Lipofectamine 2000 complex was removed and replaced with complete DMEM for an additional 18-24h. Cells were then infected with *A. phagocytophilum* MOI 50 or *B. burgdorferi* at an MOI of 200 or left uninfected overnight. The following day, D-luciferin potassium salt (RPI, L37060) was added to each well at a final concentration of 5mg/ml and luminescence measured. Data are graphed as relative light units (RLU) normalized to uninfected controls ± SEM.

Gene expression analysis of whole ticks

Gene expression profiling of whole ticks was performed on flat, unfed nymphs that were infected with *A. phagocytophilum* or *B. burgdorferi* as larvae. Individual ticks were snap frozen in liquid nitrogen and mechanically pulverized prior to the addition of TRIzol. RNA extraction and qRT-PCR analysis was performed as described above with primers listed in Supplemental Table 1. Gene expression levels were measured by qRT-PCR and normalized to uninfected controls. Data are expressed as means ± SEM.

RNAi silencing and analysis of whole ticks

RNAi silencing in *I. scapularis* larvae was performed as described previously[20]. Briefly, approximately 150 larvae were transferred to a 1.5ml tube with 40µl of siRNA or scrambled controls and incubated overnight at 15°C. Larvae were then dried and allowed to recover overnight under normal maintenance conditions prior to being placed onto mice the following day. Larvae were allowed to feed to repletion and frozen at three time points: immediately following collection, after resting (7d for *A. phagocytophilum*, 14d for *B. burgdorferi*), and after molting into nymphs. Replete larvae were weighed in groups of three to assess feeding efficiency before being processed individually, as described above. qRT-PCR analysis was performed with the use of a standard curve to generate absolute numbers of the target sequences. Primers used to generate the plasmids used in the standard curves are the same as the primers used to measure target levels (Supplemental Table 1), with the exception of *A. phagocytophilum 16S*.

Protein alignments and modeling

I. scapularis proteins were identified using NCBI (National Center for Biotechnology Information) protein BLAST and querying the tick genome with human protein sequences for PERK (NP_004827.4) and Nrf2 (NP_001138884.1). Alignments were visualized with JalView[97]. Physiochemical property conservation between amino acids is indicated by shading. AlphaFold[98,99] was used to model the protein structure of *Ixodes* Nrf2 and align it to the human Nrf2 protein structure. Alignments were visualized with UCSF ChimeraX[100].

Statistical analysis

In vitro experiments were performed with 3-5 replicates. *In vivo* experiments used at least 10-20 ticks. Data were expressed as means ± SEM and analyzed with either an unpaired Student's t-test or Welch's t-test. Calculations and graphs were created with GraphPad Prism. A P-value of < 0.05 was considered statistically significant.

REFERENCES

1. WHO | Vector-borne diseases. *WHO* http://www.who.int/mediacentre/factsheets/fs387/en/.

2. Paddock, C. D., Lane, R. S., Staples, J. E. & Labruna, M. B. *CHANGING PARADIGMS FOR TICK-BORNE DISEASES IN THE AMERICAS*. *Global Health Impacts of Vector-Borne Diseases: Workshop Summary* (National Academies Press (US), 2016).

3. *Critical Needs and Gaps in Understanding Prevention, Amelioration, and Resolution of Lyme and Other Tick-Borne Diseases: The Short-Term and Long-Term Outcomes: Workshop Report*. (National Academies Press, 2011). doi:10.17226/13134.

4. Jongejan, F. & Uilenberg, G. The global importance of ticks. *Parasitology* **129**, S3–S14 (2004).

5. Park, J. M., Oliva Chávez, A. S. & Shaw, D. K. Ticks: More Than Just a Pathogen Delivery Service. *Frontiers in Cellular and Infection Microbiology* **11**, (2021).

6. Adegoke, A., Ribeiro, J. M. C., Brown, S., Smith, R. C. & Karim, S. Rickettsia parkeri hijacks tick hemocytes to manipulate cellular and humoral transcriptional responses. *Frontiers in Immunology* **14**, (2023).

7. Liu, L. *et al.* Ixodes scapularis salivary gland protein P11 facilitates migration of Anaplasma phagocytophilum from the tick gut to salivary glands. *EMBO Rep* **12**, 1196–1203 (2011).

8. Johns, R. *et al.* Contrasts in Tick Innate Immune Responses to Borrelia burgdorferi Challenge: Immunotolerance in Ixodes scapularis Versus Immunocompetence in Dermacentor variabilis (Acari: Ixodidae). *Journal of Medical Entomology* **38**, 99–107 (2001).

9. Rittig, M. G. *et al.* Phagocytes from both vertebrate and invertebrate species use “coiling” phagocytosis. *Developmental & Comparative Immunology* **20**, 393–406 (1996).

10. Shaw, D. K. *et al.* Infection-derived lipids elicit an immune deficiency circuit in arthropods. *Nature Communications* **8**, ncomms14401 (2017).

11. Carroll, E. E. M. *et al.* p47 licenses activation of the immune deficiency pathway in the tick Ixodes scapularis. *PNAS* **116**, 205–210 (2019).

12. Rosa, R. D. *et al.* Exploring the immune signalling pathway-related genes of the cattle tick Rhipicephalus microplus: From molecular characterization to transcriptional profile upon microbial challenge. *Dev. Comp. Immunol.* **59**, 1–14 (2016).

13. Smith, A. A. & Pal, U. Immunity-related genes in Ixodes scapularis--perspectives from genome information. *Front Cell Infect Microbiol* **4**, 116 (2014).

14. Liu, L. *et al.* Ixodes scapularis JAK-STAT Pathway Regulates Tick Antimicrobial Peptides, Thereby Controlling the Agent of Human Granulocytic Anaplasmosis. *J Infect Dis.* **206**, 1233–1241 (2012).

15. Smith, A. A. *et al.* Cross-Species Interferon Signaling Boosts Microbicidal Activity within the Tick Vector. *Cell Host & Microbe* **20**, 91–98 (2016).

16. Rana, V. S. *et al.* Dome1–JAK–STAT signaling between parasite and host integrates vector immunity and development. *Science* **379**, eabl3837 (2023).

17. O'Neal, A. J. *et al.* Croquemort elicits activation of the immune deficiency pathway in ticks. *Proceedings of the National Academy of Sciences* **120**, e2208673120 (2023).

18. Gulia-Nuss, M. *et al.* Genomic insights into the Ixodes scapularis tick vector of Lyme disease. *Nat Commun* **7**, 10507 (2016).

19. Palmer, W. J. & Jiggins, F. M. Comparative Genomics Reveals the Origins and Diversity of Arthropod Immune Systems. *Mol. Biol. Evol.* **32**, 2111–2129 (2015).

20. Sidak-Loftis, L. C. *et al.* The Unfolded-Protein Response Triggers the Arthropod Immune Deficiency Pathway. *mBio* **13**, e00703-22 (2022).

21. Rosche, K. L., Sidak-Loftis, L. C., Hurtado, J., Fisk, E. A. & Shaw, D. K. Arthropods Under Pressure: Stress Responses and Immunity at the Pathogen-Vector Interface. *Front. Immunol.* **11**, (2021).

22. Grootjans, J., Kaser, A., Kaufman, R. J. & Blumberg, R. S. The unfolded protein response in immunity and inflammation. *Nat. Rev. Immunol.* **16**, 469–484 (2016).

23. Hetz, C. The unfolded protein response: controlling cell fate decisions under ER stress and beyond. *Nat Rev Mol Cell Biol* **13**, 89–102 (2012).

24. Schröder, M. & Kaufman, R. J. The mammalian unfolded protein response. *Annu. Rev. Biochem.* **74**, 739–789 (2005).

25. Casadevall, A. & Pirofski, L. Host-Pathogen Interactions: The Attributes of Virulence. *J Infect Dis* **184**, 337–344 (2001).

26. Pakos-Zebrucka, K. *et al.* The integrated stress response. *EMBO reports* **17**, 1374–1395 (2016).

27. Harding, H. P. *et al.* An Integrated Stress Response Regulates Amino Acid Metabolism and Resistance to Oxidative Stress. *Molecular Cell* **11**, 619–633 (2003).

595 28. Taniuchi, S., Miyake, M., Tsugawa, K., Oyadomari, M. & Oyadomari, S. Integrated
596 stress response of vertebrates is regulated by four eIF2α kinases. *Scientific*
597 *Reports* **6**, 32886 (2016).

598 29. Donnelly, N., Gorman, A. M., Gupta, S. & Samali, A. The eIF2α kinases: their
599 structures and functions. *Cell. Mol. Life Sci.* **70**, 3493–3511 (2013).

600 30. Ohoka, N., Yoshii, S., Hattori, T., Onozaki, K. & Hayashi, H. TRB3, a novel ER
601 stress-inducible gene, is induced via ATF4–CHOP pathway and is involved in cell
602 death. *The EMBO Journal* **24**, 1243–1255 (2005).

603 31. Han, J. *et al.* ER-stress-induced transcriptional regulation increases protein
604 synthesis leading to cell death. *Nat Cell Biol* **15**, 481–490 (2013).

605 32. Sidrauski, C., McGeachy, A. M., Ingolia, N. T. & Walter, P. The small molecule
606 ISRIB reverses the effects of eIF2α phosphorylation on translation and stress
607 granule assembly. *eLife* **4**, e05033 (2015).

608 33. Long, K., Boyce, M., Lin, H., Yuan, J. & Ma, D. Structure–activity relationship
609 studies of salubrinal lead to its active biotinylated derivative. *Bioorganic &*
610 *Medicinal Chemistry Letters* **15**, 3849–3852 (2005).

611 34. Boyce, M. *et al.* A Selective Inhibitor of eIF2α Dephosphorylation Protects Cells
612 from ER Stress. *Science* **307**, 935–939 (2005).

613 35. Hodzic, E. *et al.* Acquisition and transmission of the agent of human granulocytic
614 ehrlichiosis by Ixodes scapularis ticks. *J. Clin. Microbiol.* **36**, 3574–3578 (1998).

615 36. Abraham, N. M. *et al.* Pathogen-mediated manipulation of arthropod microbiota to
616 promote infection. *Proc Natl Acad Sci U S A* **114**, E781–E790 (2017).

617 37. Narasimhan, S. *et al.* Gut microbiota of the tick vector Ixodes scapularis modulate
618 colonization of the lyme disease spirochete. *Cell Host Microbe* **15**, 58–71 (2014).

619 38. Narasimhan, S. *et al.* Modulation of the tick gut milieu by a secreted tick protein
620 favors Borrelia burgdorferi colonization. *Nat Commun* **8**, 184 (2017).

621 39. Piesman, J., Oliver, J. R. & Sinsky, R. J. Growth kinetics of the Lyme disease
622 spirochete (Borrelia burgdorferi) in vector ticks (Ixodes dammini). *Am. J. Trop.*
623 *Med. Hyg.* **42**, 352–357 (1990).

624 40. Pal, U., Kitsou, C., Drecktrah, D., Yaş, Ö. B. & Fikrig, E. Interactions Between
625 Ticks and Lyme Disease Spirochetes. *Curr Issues Mol Biol* **42**, 113–144 (2021).

626 41. Anderson, J. M., Sonenshine, D. E. & Valenzuela, J. G. Exploring the mialome of
627 ticks: an annotated catalogue of midgut transcripts from the hard tick,
628 Dermacentor variabilis (Acari: Ixodidae). *BMC Genomics* **9**, 552 (2008).

629 42. Ebnet, K., Brown, K. D., Siebenlist, U. K., Simon, M. M. & Shaw, S. Borrelia
630 burgdorferi activates nuclear factor-kappa B and is a potent inducer of chemokine

631 and adhesion molecule gene expression in endothelial cells and fibroblasts. *J*
632 *Immunol* **158**, 3285–3292 (1997).

633 43. Lee, H. C., Kioi, M., Han, J., Puri, R. K. & Goodman, J. L. Anaplasma
634 phagocytophilum-induced gene expression in both human neutrophils and HL-60
635 cells. *Genomics* **92**, 144–151 (2008).

636 44. Dumler, J. S., Lichay, M., Chen, W.-H., Rennoll-Bankert, K. E. & Park, J.
637 Anaplasma phagocytophilum Activates NF-κB Signaling via Redundant Pathways.
638 *Frontiers in Public Health* **8**, (2020).

639 45. Sarkar, A. *et al.* Infection with Anaplasma phagocytophilum Activates the
640 Phosphatidylinositol 3-Kinase/Akt and NF-κB Survival Pathways in Neutrophil
641 Granulocytes. *Infection and Immunity* **80**, 1615–1623 (2012).

642 46. Moi, P., Chan, K., Asunis, I., Cao, A. & Kan, Y. W. Isolation of NF-E2-related
643 factor 2 (Nrf2), a NF-E2-like basic leucine zipper transcriptional activator that
644 binds to the tandem NF-E2/AP1 repeat of the beta-globin locus control region.
645 *Proceedings of the National Academy of Sciences* **91**, 9926–9930 (1994).

646 47. Hayes, J. D. & Dinkova-Kostova, A. T. The Nrf2 regulatory network provides an
647 interface between redox and intermediary metabolism. *Trends in Biochemical*
648 *Sciences* **39**, 199–218 (2014).

649 48. Sarcinelli, C. *et al.* ATF4-Dependent NRF2 Transcriptional Regulation Promotes
650 Antioxidant Protection during Endoplasmic Reticulum Stress. *Cancers (Basel)* **12**,
651 569 (2020).

652 49. Cullinan, S. B. & Diehl, J. A. PERK-dependent Activation of Nrf2 Contributes to
653 Redox Homeostasis and Cell Survival following Endoplasmic Reticulum Stress*.
654 *Journal of Biological Chemistry* **279**, 20108–20117 (2004).

655 50. He, C. H. *et al.* Identification of Activating Transcription Factor 4 (ATF4) as an
656 Nrf2-interacting Protein: IMPLICATION FOR HEME OXYGENASE-1 GENE
657 REGULATION*. *Journal of Biological Chemistry* **276**, 20858–20865 (2001).

658 51. Itoh, K. *et al.* An Nrf2/small Maf heterodimer mediates the induction of phase II
659 detoxifying enzyme genes through antioxidant response elements. *Biochem*
660 *Biophys Res Commun* **236**, 313–322 (1997).

661 52. Rushmore, T. H., Morton, M. R. & Pickett, C. B. The antioxidant responsive
662 element. Activation by oxidative stress and identification of the DNA consensus
663 sequence required for functional activity. *J Biol Chem* **266**, 11632–11639 (1991).

664 53. De, S. *et al.* A high-quality Ixodes scapularis genome advances tick science. *Nat*
665 *Genet* **55**, 301–311 (2023).

666 54. Sengoku, T. *et al.* Structural basis of transcription regulation by CNC family
667 transcription factor, Nrf2. *Nucleic Acids Research* **50**, 12543–12557 (2022).

55. Lin, M. & Rikihisa, Y. Degradation of p22phox and inhibition of superoxide generation by Ehrlichia chaffeensis in human monocytes. *Cellular Microbiology* **9**, 861–874 (2007).

56. Boylan, J. A. & Gherardini, F. C. Determining the cellular targets of reactive oxygen species in Borrelia burgdorferi. *Methods Mol. Biol* **431**, 213–221 (2008).

57. Hyde, J. A., Shaw, D. K., Smith Iii, R., Trzeciakowski, J. P. & Skare, J. T. The BosR regulatory protein of Borrelia burgdorferi interfaces with the RpoS regulatory pathway and modulates both the oxidative stress response and pathogenic properties of the Lyme disease spirochete. *Mol. Microbiol.* **74**, 1344–1355 (2009).

58. Hyde, J. A., Shaw, D. K., Smith, R., Trzeciakowski, J. P. & Skare, J. T. Characterization of a Conditional bosR Mutant in Borrelia burgdorferi. *Infect Immun* **78**, 265–274 (2010).

59. Mott, J. & Rikihisa, Y. Human Granulocytic Ehrlichiosis Agent Inhibits Superoxide Anion Generation by Human Neutrophils. *Infection and Immunity* **68**, 6697–6703 (2000).

60. Carlyon, J. A. & Fikrig, E. Invasion and survival strategies of Anaplasma phagocytophilum. *Cellular Microbiology* **5**, 743–754 (2003).

61. Carlyon, J. A., Latif, D. A., Pypaert, M., Lacy, P. & Fikrig, E. Anaplasma phagocytophilum Utilizes Multiple Host Evasion Mechanisms To Thwart NADPH Oxidase-Mediated Killing during Neutrophil Infection. *Infection and Immunity* **72**, 4772–4783 (2004).

62. Alberdi, P. *et al.* The redox metabolic pathways function to limit Anaplasma phagocytophilum infection and multiplication while preserving fitness in tick vector cells. *Sci Rep* **9**, 13236 (2019).

63. Ramsey, M. E. *et al.* A high-throughput genetic screen identifies previously uncharacterized Borrelia burgdorferi genes important for resistance against reactive oxygen and nitrogen species. *PLOS Pathogens* **13**, e1006225 (2017).

64. Bourret, T. J. *et al.* The Nucleotide Excision Repair Pathway Protects Borrelia burgdorferi from Nitrosative Stress in Ixodes scapularis Ticks. *Frontiers in Microbiology* **7**, (2016).

65. Bourret, T. J., Boylan, J. A., Lawrence, K. A. & Gherardini, F. C. Nitrosative damage to free and zinc-bound cysteine thiols underlies nitric oxide toxicity in wild-type Borrelia burgdorferi. *Molecular Microbiology* **81**, 259–273 (2011).

66. Troxell, B. *et al.* Pyruvate Protects Pathogenic Spirochetes from H2O2 Killing. *PLOS ONE* **9**, e84625 (2014).

67. Yang, X., Smith, A. A., Williams, M. S. & Pal, U. A Dityrosine Network Mediated by Dual Oxidase and Peroxidase Influences the Persistence of Lyme Disease Pathogens within the Vector. *J. Biol. Chem.* **289**, 12813–12822 (2014).

68. Narasimhan, S. *et al.* A Tick Antioxidant Facilitates the Lyme Disease Agent's Successful Migration from the Mammalian Host to the Arthropod Vector. *Cell Host Microbe* **2**, 7–18 (2007).

69. Park, J. M. *et al.* An Anaplasma phagocytophilum T4SS effector, AteA, is essential for tick infection. 2023.02.06.527355 Preprint at https://doi.org/10.1101/2023.02.06.527355 (2023).

70. Shaw, D. K. *et al.* Vector Immunity and Evolutionary Ecology: The Harmonious Dissonance. *Trends in Immunology* **39**, 862–873 (2018).

71. Ding, W., Yang, L., Zhang, M. & Gu, Y. Reactive oxygen species-mediated endoplasmic reticulum stress contributes to aldosterone-induced apoptosis in tubular epithelial cells. *Biochemical and Biophysical Research Communications* **418**, 451–456 (2012).

72. Liu, Z.-W. *et al.* Protein kinase RNA- like endoplasmic reticulum kinase (PERK) signaling pathway plays a major role in reactive oxygen species (ROS)- mediated endoplasmic reticulum stress- induced apoptosis in diabetic cardiomyopathy. *Cardiovascular Diabetology* **12**, 158 (2013).

73. Durante, W., Johnson, F. K. & Johnson, R. A. ARGINASE: A CRITICAL REGULATOR OF NITRIC OXIDE SYNTHESIS AND VASCULAR FUNCTION. *Clin Exp Pharmacol Physiol* **34**, 906–911 (2007).

74. Villar, M. *et al.* Integrated Metabolomics, Transcriptomics and Proteomics Identifies Metabolic Pathways Affected by Anaplasma phagocytophilum Infection in Tick Cells. *Mol Cell Proteomics* **14**, 3154–3172 (2015).

75. Sapiro, A. L. *et al. Longitudinal map of transcriptome changes in the Lyme pathogen Borrelia burgdorferi during tick-borne transmission*. https://elifesciences.org/reviewed-preprints/86636v1 (2023) doi:10.7554/eLife.86636.1.

76. Tonelli, C., Chio, I. I. C. & Tuveson, D. A. Transcriptional Regulation by Nrf2. *Antioxid Redox Signal* **29**, 1727–1745 (2018).

77. Gorrini, C., Harris, I. S. & Mak, T. W. Modulation of oxidative stress as an anticancer strategy. *Nat Rev Drug Discov* **12**, 931–947 (2013).

78. Budachetri, K. & Karim, S. An insight into the functional role of Thioredoxin reductase, a selenoprotein, in maintaining normal native microbiota in the Gulf-Coast tick (Amblyomma maculatum). *Insect Mol Biol* **24**, 570–581 (2015).

79. Budachetri, K., Kumar, D. & Karim, S. Catalase is a determinant of the colonization and transovarial transmission of Rickettsia parkeri in the Gulf Coast tick Amblyomma maculatum. *Insect Molecular Biology* **26**, 414–419 (2017).

80. Kumar, D., Embers, M., Mather, T. N. & Karim, S. Is selenoprotein K required for Borrelia burgdorferi infection within the tick vector Ixodes scapularis? *Parasites & Vectors* **12**, 289 (2019).

81. Hernandez, E. P., Talactac, M. R., Vitor, R. J. S., Yoshii, K. & Tanaka, T. An Ixodes scapularis glutathione S-transferase plays a role in cell survival and viability during Langat virus infection of a tick cell line. *Acta Tropica* **214**, 105763 (2021).

82. Crispell, G., Budachetri, K. & Karim, S. Rickettsia parkeri colonization in Amblyomma maculatum: the role of superoxide dismutases. *Parasites & Vectors* **9**, 291 (2016).

83. Adamson, S. W., Browning, R. E., Budachetri, K., Ribeiro, J. M. C. & Karim, S. Knockdown of Selenocysteine-Specific Elongation Factor in Amblyomma maculatum Alters the Pathogen Burden of Rickettsia parkeri with Epigenetic Control by the Sin3 Histone Deacetylase Corepressor Complex. *PLOS ONE* **8**, e82012 (2013).

84. Kocan, K. M. *et al.* Silencing of genes involved in Anaplasma marginale-tick interactions affects the pathogen developmental cycle in Dermacentor variabilis. *BMC Developmental Biology* **9**, 42 (2009).

85. Kumar, D., Budachetri, K., Meyers, V. C. & Karim, S. Assessment of tick antioxidant responses to exogenous oxidative stressors and insight into the role of catalase in the reproductive fitness of the Gulf Coast tick, Amblyomma maculatum. *Insect Molecular Biology* **25**, 283–294 (2016).

86. Budachetri, K. *et al.* The tick endosymbiont Candidatus Midichloria mitochondrii and selenoproteins are essential for the growth of Rickettsia parkeri in the Gulf Coast tick vector. *Microbiome* **6**, 141 (2018).

87. DeSouza-Vieira, T. *et al.* Heme Oxygenase-1 Induction by Blood-Feeding Arthropods Controls Skin Inflammation and Promotes Disease Tolerance. *Cell Reports* **33**, 108317 (2020).

88. Perner, J. *et al.* Acquisition of exogenous haem is essential for tick reproduction. *eLife* **5**, e12318.

89. Shaw, D. K. *et al.* Infection-derived lipids elicit an immune deficiency circuit in arthropods. *Nature Communications* **8**, 14401 (2017).

90. Sukumaran, B. *et al.* Rip2 contributes to host defense against Anaplasma phagocytophilum infection. *FEMS Immunol Med Microbiol* **66**, 211–219 (2012).

776 91. Pedra, J. H. F. *et al.* ASC/PYCARD and Caspase-1 Regulate the IL-18/IFN-γ Axis
777 during Anaplasma phagocytophilum Infection1. *The Journal of Immunology* **179**,
778 4783–4791 (2007).

779 92. Labandeira-Rey, M. & Skare, J. T. Decreased Infectivity in Borrelia burgdorferi
780 Strain B31 Is Associated with Loss of Linear Plasmid 25 or 28-1. *Infection and*
781 *Immunity* **69**, 446–455 (2001).

782 93. James, A. E., Rogovskyy, A. S., Crowley, M. A. & Bankhead, T. Characterization
783 of a DNA Adenine Methyltransferase Gene of Borrelia hermsii and Its
784 Dispensability for Murine Infection and Persistence. *PLOS ONE* **11**, e0155798
785 (2016).

786 94. Bankhead, T. & Chaconas, G. The role of VlsE antigenic variation in the Lyme
787 disease spirochete: persistence through a mechanism that differs from other
788 pathogens. *Molecular Microbiology* **65**, 1547–1558 (2007).

789 95. Severo, M. S. *et al.* The E3 Ubiquitin Ligase XIAP Restricts Anaplasma
790 phagocytophilum Colonization of Ixodes scapularis Ticks. *J Infect Dis* **208**, 1830–
791 1840 (2013).

792 96. Abuaita, B. H., Schultz, T. L. & O'Riordan, M. X. Mitochondria-Derived Vesicles
793 Deliver Antimicrobial Reactive Oxygen Species to Control Phagosome-Localized
794 Staphylococcus aureus. *Cell Host & Microbe* **24**, 625-636.e5 (2018).

795 97. Waterhouse, A. M., Procter, J. B., Martin, D. M. A., Clamp, M. & Barton, G. J.
796 Jalview Version 2—a multiple sequence alignment editor and analysis workbench.
797 *Bioinformatics* **25**, 1189–1191 (2009).

798 98. Jumper, J. *et al.* Highly accurate protein structure prediction with AlphaFold.
799 *Nature* **596**, 583–589 (2021).

800 99. Varadi, M. *et al.* AlphaFold Protein Structure Database: massively expanding the
801 structural coverage of protein-sequence space with high-accuracy models.
802 *Nucleic Acids Research* **50**, D439–D444 (2022).

803 100. Pettersen, E. F. *et al.* UCSF ChimeraX: Structure visualization for researchers,
804 educators, and developers. *Protein Science* **30**, 70–82 (2021).

805

FIGURE LEGENDS

Figure 1 | Tick-borne pathogens induce eIF2α-regulated stress responses in infected, unfed nymphs. (**A**) Graphic representation of IRE1α-TRAF2 signaling and the Integrated Stress Response pathways in *Ixodes* ticks. (**B-I**) Gene expression in flat, unfed *I. scapularis* nymphs that are either uninfected (-), *A. phagocytophilum*-infected (*A.p.*), or *B. burgdorferi*-infected (*B.b.*). Each data point is representative of 1 nymph. Gene expression was quantified by qRT-PCR using primers listed in Supplemental Table 1. Student's t-test. *P < 0.05. (**J**) Phosphorylated eIF2α (36 kDa) immunoblot against ISE6 tick cells that were either uninfected (-), infected for 24 hrs (*A. phagocytophilum*: *A.p.*; *B. burgdorferi*: *B.b.;* MOI 50), or treated with the eIF2α phosphorylation inhibitor ISRIB for 1 hr prior to infection (24 hrs). β-actin was probed as an internal loading control (45 kDa). Immunoblots are representative of 2 biological replicates. See also Supplemental Figure 1.

Figure 2 | The PERK-eIF2α-ATF4 axis promotes *A. phagocytophilum* infection in tick cells. (**A-B**) ISE6 tick cells (1 x 10^6) were pretreated with ISRIB (**A**) or salubrinal (**B**) at the indicated concentrations for 1 hr prior to infection with *A. phagocytophilum* for 18 hrs (MOI 50). (**C-G**) IDE12 tick cells (1 x 10^6) were treated with silencing RNAs (siRNA) against indicated genes or scrambled RNA controls (scRNA) for 24 hrs prior to infection with *A. phagocytophilum* (MOI 50) for 18 hrs. *A. phagocytophilum* burden and gene silencing for *eIF2α* (**C**), *ATF4* (**D**), *GCN2* (**E**), *HRI* (**F**), and *PERK* (**G**) were measured by qRT-PCR. Data are representative of at least five biological replicates with at least two technical replicates. Error bars show SEM, *P < 0.05 (Student's t-test). scRNA, scrambled RNA; siRNA, small interfering RNA.

Figure 3 | The PERK pathway supports *A. phagocytophilum in vivo.* *I. scapularis* larvae were immersed overnight in siRNA targeting *PERK* (**A-D**), *eIF2α* (**E-H**), or *ATF4* (**I-L**) and fed on *A. phagocytophilum*-infected mice. Silencing efficiency (**A, E, I**) and bacterial burden were assessed at three time intervals by qRT-PCR: immediately following repletion (**B, F, J**), one-week post-repletion (**C, G, K**), and after ticks molted to nymphs (**D, H, L**). Data are representative of 10-20 ticks and at least two experimental replicates. Each point represents one tick, with two technical replicates. Error bars show SEM, *p < 0.05 (Welch's t-test). NS, non-significant. scRNA, scrambled RNA, siRNA, small interfering RNA.

Figure 4 | *In vivo B. burgdorferi* colonization and persistence through the molt is supported by the PERK pathway. *PERK* (**A-D**), *eIF2α* (**E-H**), or *ATF4* (**I-L**) were silenced in *I. scapularis* larvae by immersing ticks in siRNA overnight. Recovered ticks were fed on *B. burgdorferi*-infected mice. Silencing efficiency (**A, E, I**) and bacterial burden were assessed at three time intervals by qRT-PCR: immediately following repletion (**B, F, J**), two weeks post-repletion (**C, G, K**), and after ticks molted to nymphs (**D, H, L**). Data are representative of 10-20 ticks and at least two experimental replicates. Each point represents one tick, with two technical replicates. Error bars show SEM, *P < 0.05 (Welch's t-test). scRNA, scrambled RNA, siRNA, small interfering RNA.

Figure 5 | Infection triggers an Nrf2-regulated antioxidant response in ticks that promotes pathogen survival. (**A-B**) HEK293T cells (1 x 10^4) were transfected with luciferase reporter vectors for assaying activity of ER stress transcription factors XBP1, NF-κB, CHOP, SREBP1, and NRF2 or were untransfected (-). Cells were then infected with *A. phagocytophilum* (*A.p.*) (**A**) or *B. burgdorferi* (*B.b.*) (**B**). After 24 hrs, D-luciferase

was added and luminescence was measured as relative luminescence units (RLU). Measurements were normalized to uninfected controls (gray bars). Luciferase assays are representative of 3-5 biological replicates with at least two experimental replicates ± SEM. Student's t-test. *P < 0.05. (**C-D**) Predicted *Ixodes* Nrf2 structure modeled with AlphaFold[98,99] (blue) and overlaid with human Nrf2 (orange) using UCSF ChimeraX[100]. The bZIP domain is indicated by a box with dashed lines. (**D**) Magnified region of the bZIP domain depicting residues that that are predicted to interact with ARE sequences in DNA promoter regions (R877, R880, R882, N885, A888, A889, R893, R895, K896). See also Supplemental Figure 2. (**E**) *Nrf2* expression levels in flat, unfed nymphs that are uninfected (-), *A. phagocytophilum*-infected (*A.p.*), or *B. burgdorferi*-infected (*B.b.*). Each data point is representative of 1 nymph. Gene expression was quantified by qRT-PCR using Nrf2 primers listed in Supplemental Table 1. Student's t-test. *P < 0.05. (**F-H**) IDE12 tick cells were treated with silencing RNAs (siRNA) targeting *nrf2* for 24 hrs prior to infection with *A. phagocytophilum* (18 hrs) (**F-G**) or *B. burgdorferi* (**H**). Gene silencing (**F-H**) and bacterial burden (**G-H**) were quantified by qRT-PCR. ROS was measured as relative fluorescent units (RFU) after 24 hrs of infection (**F**). Data are representative of at least 4-5 biological replicates and two technical replicates. Error bars show SEM, *P < 0.05 (Student's t-test). scRNA, scrambled RNA; siRNA, small interfering RNA.

Figure 6 | Antioxidant activity of the PERK-eIF2α pathway protects pathogens in ticks. (**A-D**) ROS (**A, B**) and RNS (**C, D**) measurements in ISE6 cells (1.68×10^5) untreated (-), infected (*A.p.* or *B.b.*), or pretreated with 1μM ISRIB prior to infection with *A. phagocytophilum* (ISRIB + *A.p.*) (**A, C**) or *B. burgdorferi* (ISRIB + *B.b.*) (**B, D**).

875 Fluorescence was measured at the indicated time points and is presented as RFU,
876 normalized to untreated, uninfected controls (-). (**E-F**) IDE12 cells were infected with *A.*
877 *phagocytophilum* (**E**) or *B. burgdorferi* (**F**) alone or in the presence of 5mM NAC for 24
878 hrs. (**G-H**) *perk* was silenced in IDE12 cells (1 x 10^6). Cells were infected with *A.*
879 *phagocytophilum* (**G**) or *B. burgdorferi* (**H**) alone or in the presence of 5mM NAC.
880 Silencing levels and bacterial burdens were quantified by qRT-PCR. Data are
881 representative of at least 4-5 biological replicates and two technical replicates. Error
882 bars show SEM, *P < 0.05 (Student's t-test). NAC, N-acetyl cysteine. scRNA, scrambled
883 RNA; siRNA, small interfering RNA.

884 **Figure 7 | The PERK-eIF2α-ATF4 axis promotes pathogen survival in ticks**
885 **through an Nrf2-mediated antioxidant response.** When colonizing the tick, *A.*
886 *phagocytophilum* and *B. burgdorferi* trigger the *Ixodes* IMD pathway and ROS/RNS
887 through the IRE1α-TRAF2 axis of the UPR. Tick-borne microbes persist in the tick over
888 time by stimulating the PERK branch of the UPR, which signals through eIF2α and the
889 transcription factors ATF4 and Nrf2 to trigger an antioxidant response that promotes
890 microbial survival.

ACKNOWLEDGEMENTS

We are grateful to Ulrike Munderloh (University of Minnesota) for providing ISE6 and IDE12 tick cell lines; Jon Skare (Texas A&M Health Science Center) for providing *B. burgdorferi* B31 (MSK5); BEI Resources and Oklahoma State University for *Ixodes scapularis* ticks, and Arden Baylink (Washington State University) for guidance with AlphaFold and UCSF ChimeraX. Schematics in Figures 1 and 7 were created with Biorender.com.

Funding

This work is supported by the National Institutes of Health (R21AI148578 and R21AI139772 to D.K.S.), the WSU Intramural CVM grants program, funded in part by the National Institute of Food and Agriculture and the Joseph and Barbara Mendelson Endowment Research Fund (to D.K.S.) and Washington State University, College of Veterinary Medicine. J.H. and K.A.V. are trainees supported by an Institutional T32 Training Grant from the National Institute of Allergy and Infection Diseases (T32GM008336). E.A.F. is a trainee supported by an Institutional T32 Training Grant from the National Institute of Allergy and Infection Diseases (T32AI007025). Additional support to L.C.S-L. came from The Fowler Emerging Diseases Graduate Fellowship funded by Ralph and Maree Fowler, the Kraft Graduate Scholarship, and the Poncin Fellowship. E.R-Z is a trainee supported by an Institutional Training Grant MIRA R25 ESTEEMED from the National Institute of Biomedical Imaging and Bioengineering (R25EB027606). The content is solely the responsibility of the authors and does not

necessarily represent the official views of the National Institute of Allergy and Infection Diseases or the National Institutes of Health.

Author contributions

K.L.R., J.H., and D.K.S. designed the study. K.L.R., J.H., E.A.F., K.A.V., A.L.W., L.C.S-L., S.J.W., E.R-Z., J.M.P., and D.K.S. contributed to methodology, investigation, and data analysis. All authors provided intellectual input into the study. K.L.R. and D.K.S. wrote the manuscript; all authors contributed to editing.

Figure 1 | Tick-borne pathogens induce eIF2α-regulated stress responses in infected, unfed nymphs

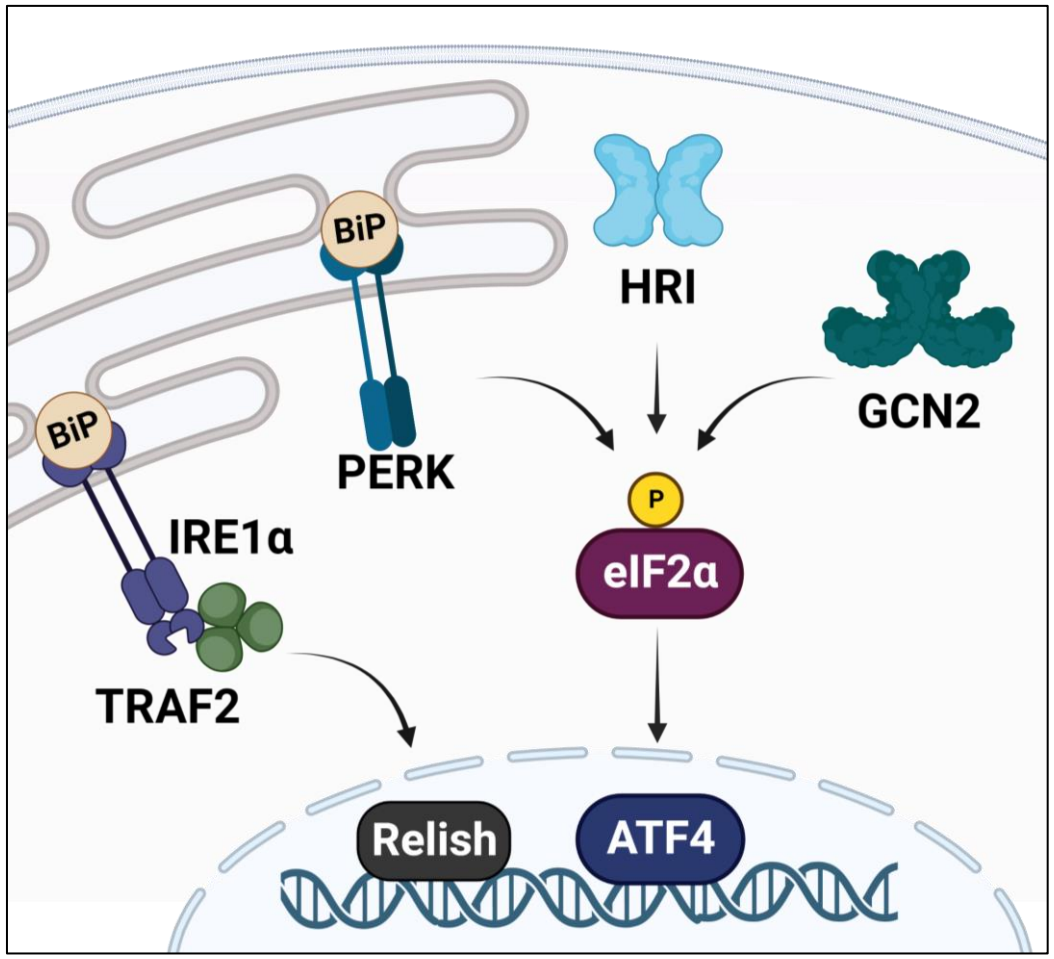

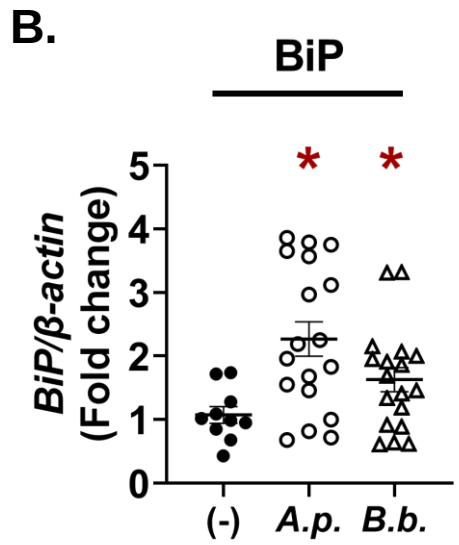

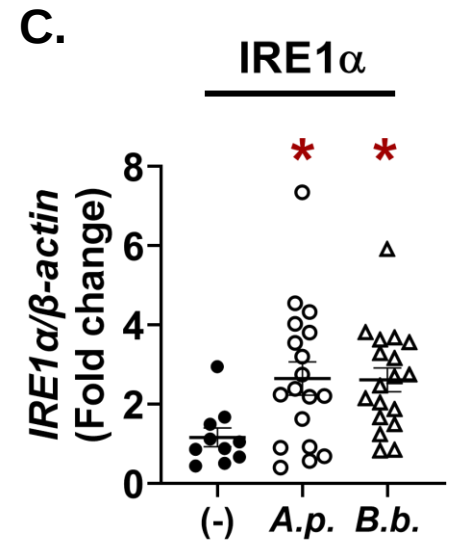

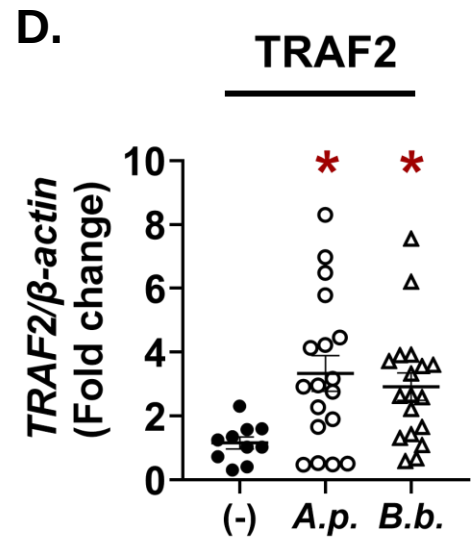

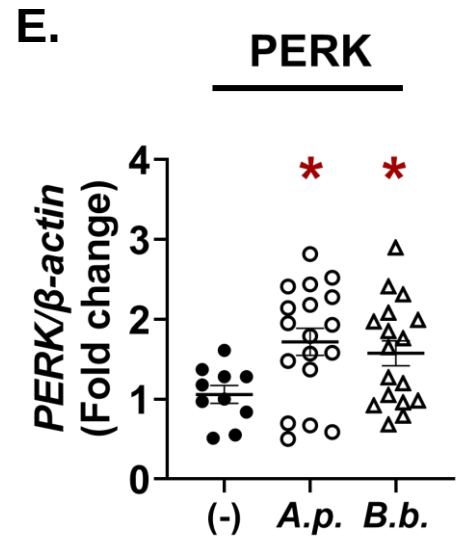

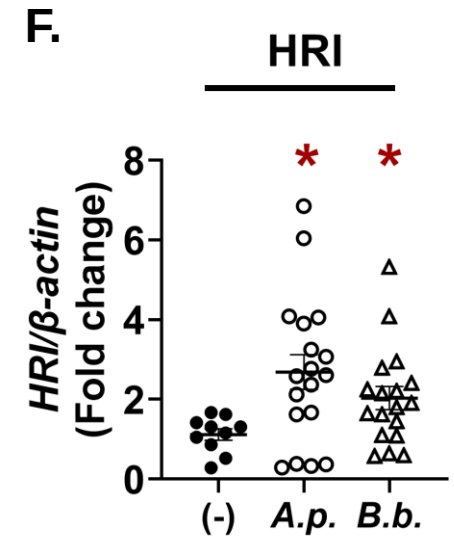

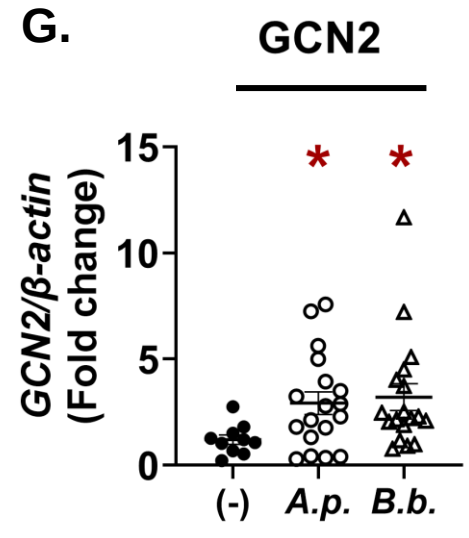

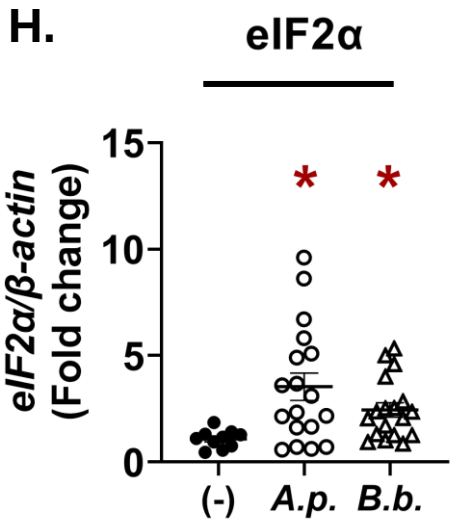

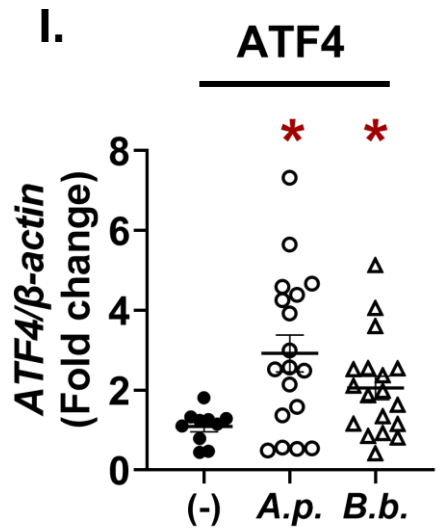

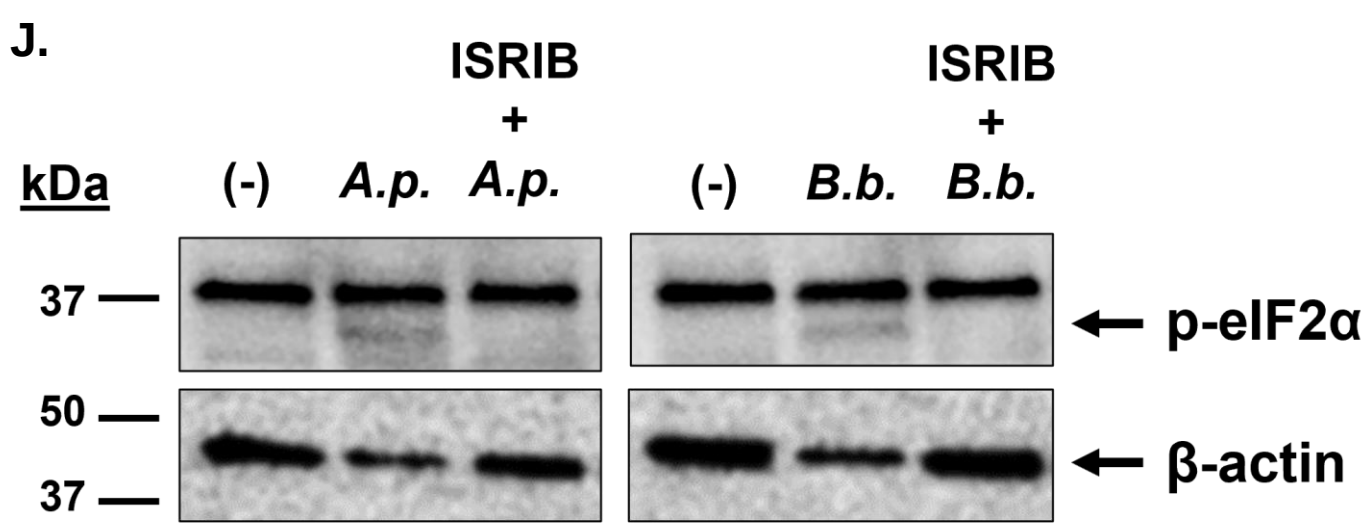

Figure 2 | The PERK-eIF2α-ATF4 axis promotes *A. phagocytophilum* infection in tick cells.

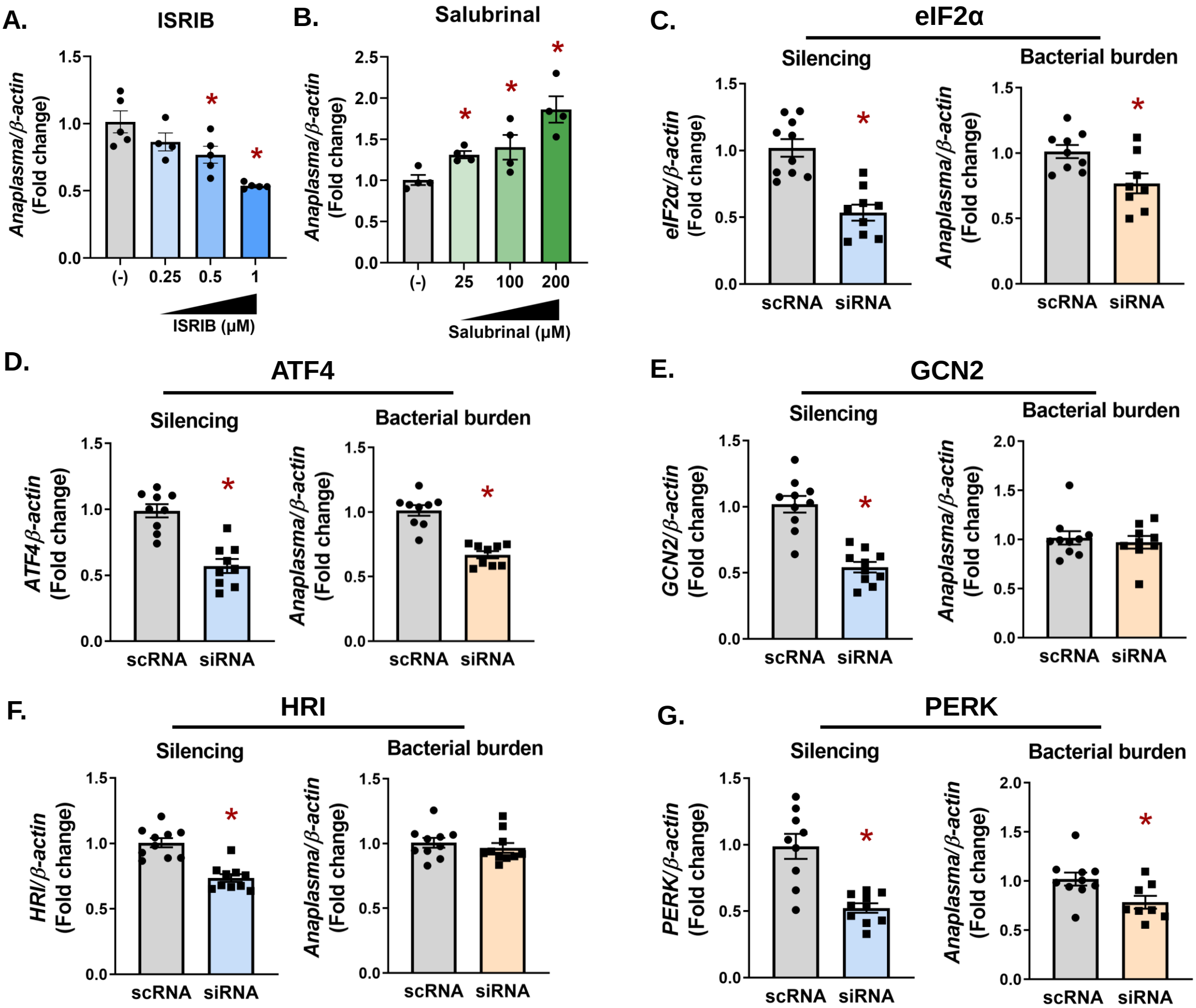

Figure 3 | The PERK pathway supports *A. phagocytophilum in vivo*

PERK

A.
Silencing
PERK/β-actin (Fold change)
scRNA siRNA
*

B.
Bacterial burden
Anaplasma/β-actin (Fold change)
scRNA siRNA
*

C.
Bacterial burden
Anaplasma/β-actin (Fold change)
scRNA siRNA
*

D.
Bacterial burden
Anaplasma/β-actin (Fold change)
scRNA siRNA
NS

eIF2α

E.
Silencing
eIF2α/β-actin (Fold change)
scRNA siRNA
*

F.
Bacterial burden
Anaplasma/β-actin (Fold change)
scRNA siRNA
*

G.
Bacterial burden
Anaplasma/β-actin (Fold change)
scRNA siRNA
*

H.
Bacterial burden
Anaplasma/β-actin (Fold change)
scRNA siRNA
*

ATF4

I.
Silencing
ATF4/β-actin (Fold change)
scRNA siRNA
*

J.
Bacterial burden
Anaplasma/β-actin (Fold change)
scRNA siRNA
*

K.
Bacterial burden
Anaplasma/β-actin (Fold change)
scRNA siRNA
*

L.
Bacterial burden
Anaplasma/β-actin (Fold change)
scRNA siRNA
NS

Figure 4 | *In vivo B. burgdorferi* colonization and persistence through the molt is supported by the PERK pathway

PERK

A. Silencing — *PERK*/*β-actin* (Fold change) — scRNA siRNA

B. Bacterial burden — *Borrelia*/*β-actin* (Fold change) — scRNA siRNA

C. Bacterial burden — *Borrelia*/*β-actin* (Fold change) — scRNA siRNA

D. Bacterial burden — *Borrelia*/*β-actin* (Fold change) — scRNA siRNA

eIF2α

E. Silencing — *eIF2α*/*β-actin* (Fold change) — scRNA siRNA

F. Bacterial burden — *Borrelia*/*β-actin* (Fold change) — scRNA siRNA

G. Bacterial burden — *Borrelia*/*β-actin* (Fold change) — scRNA siRNA

H. Bacterial burden — *Borrelia*/*β-actin* (Fold change) — scRNA siRNA

ATF4

I. Silencing — *ATF4*/*β-actin* (Fold change) — scRNA siRNA

J. Bacterial burden — *Borrelia*/*β-actin* (Fold change) — scRNA siRNA

K. Bacterial burden — *Borrelia*/*β-actin* (Fold change) — scRNA siRNA

L. Bacterial burden — *Borrelia*/*β-actin* (Fold change) — scRNA siRNA

Figure 5 | Infection triggers an Nrf2 antioxidant response that promotes pathogen survival in ticks

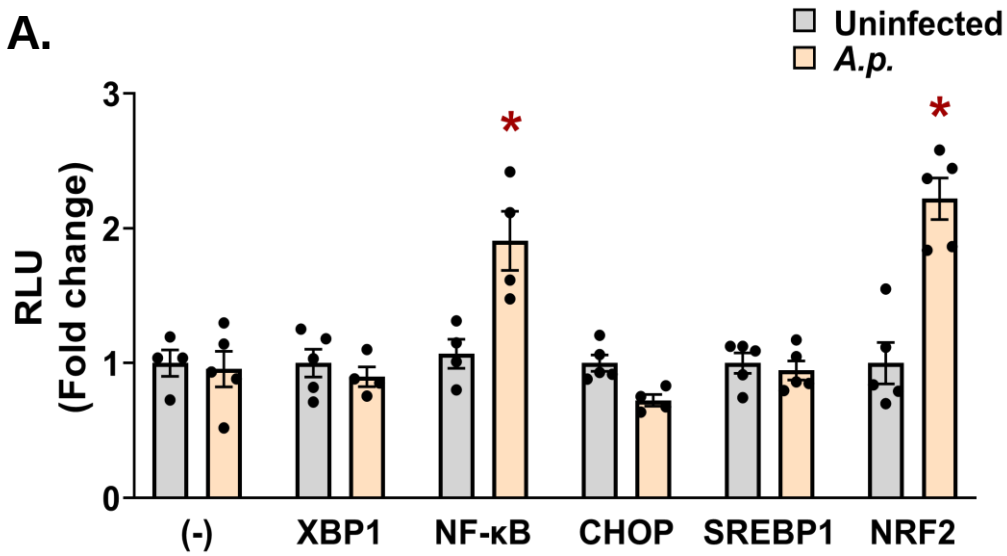

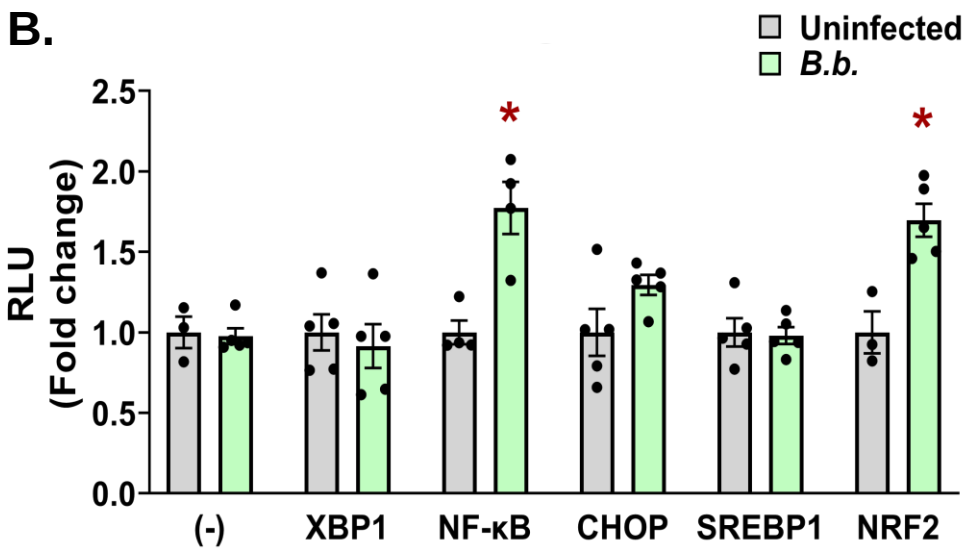

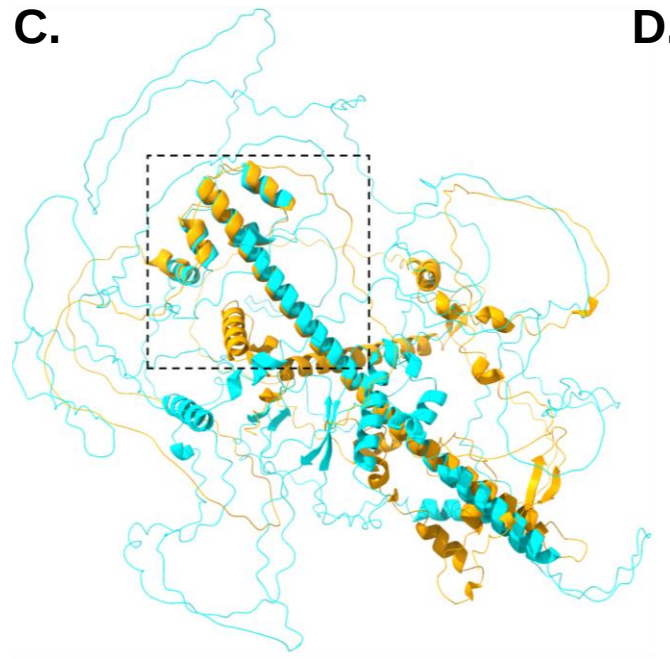

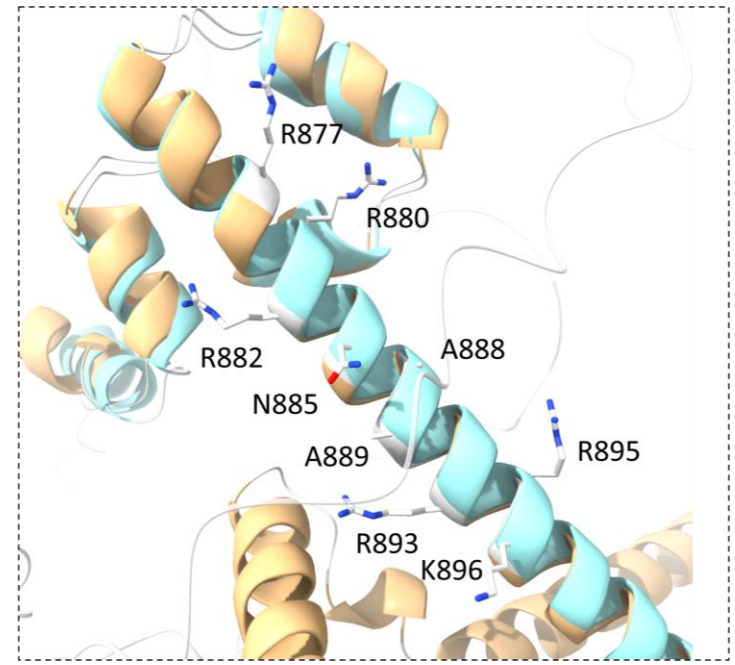

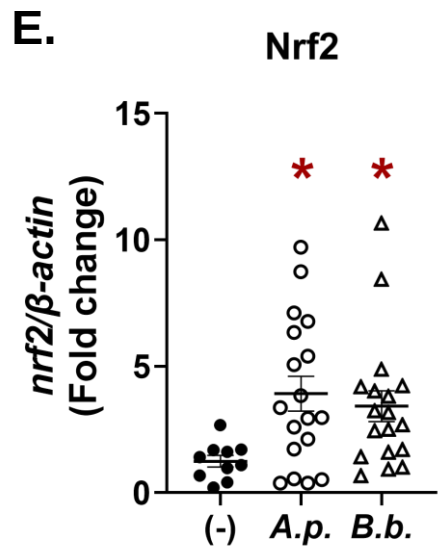

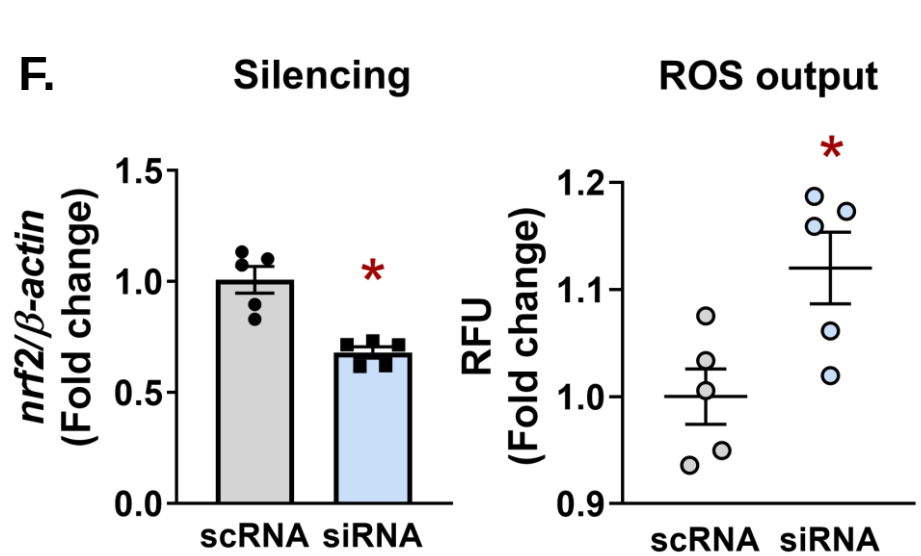

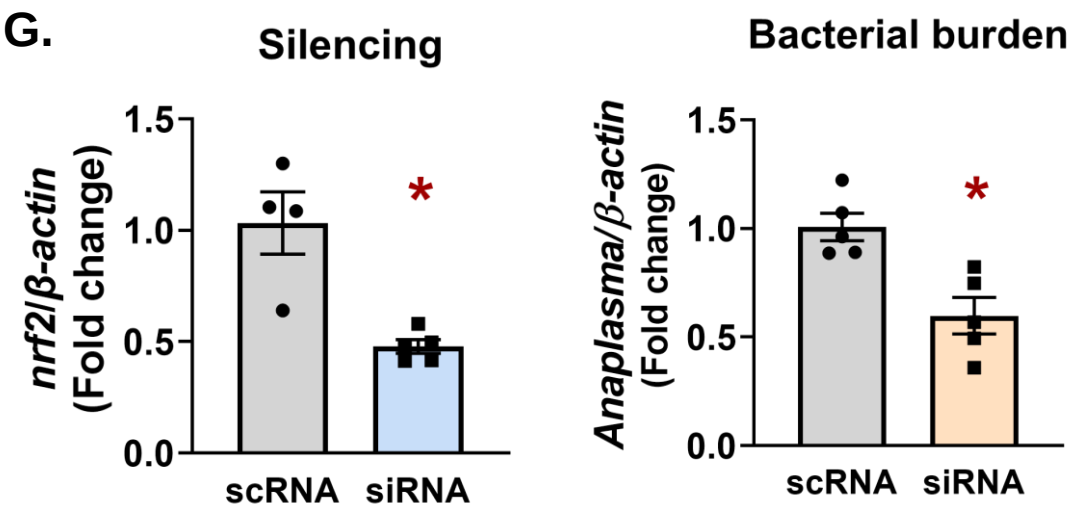

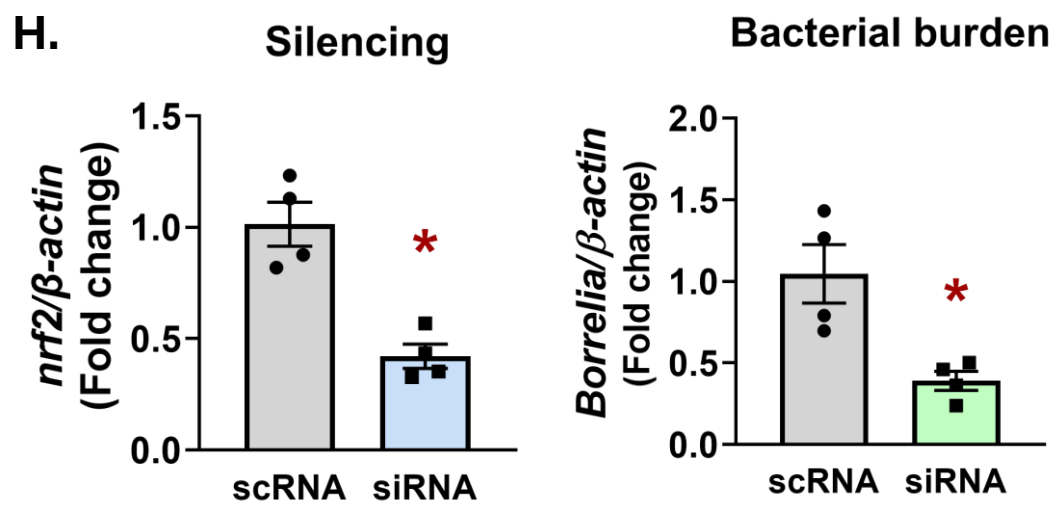

Figure 6 | Antioxidant activity of the PERK-eIF2α pathway protects pathogens in ticks

ROS

RNS

A.

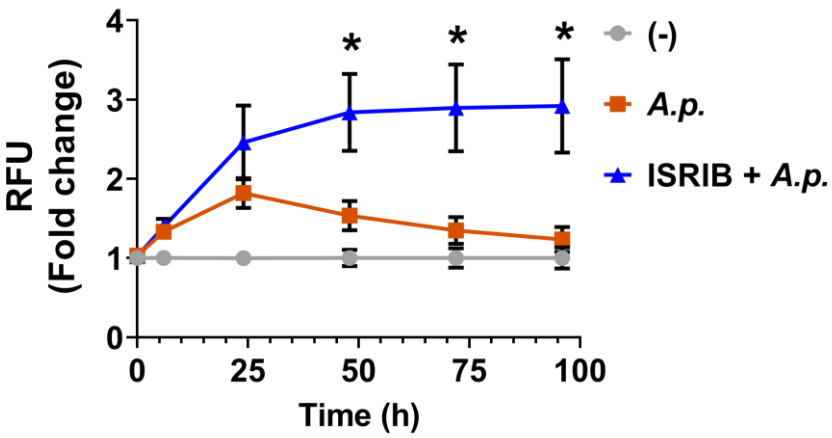

B.

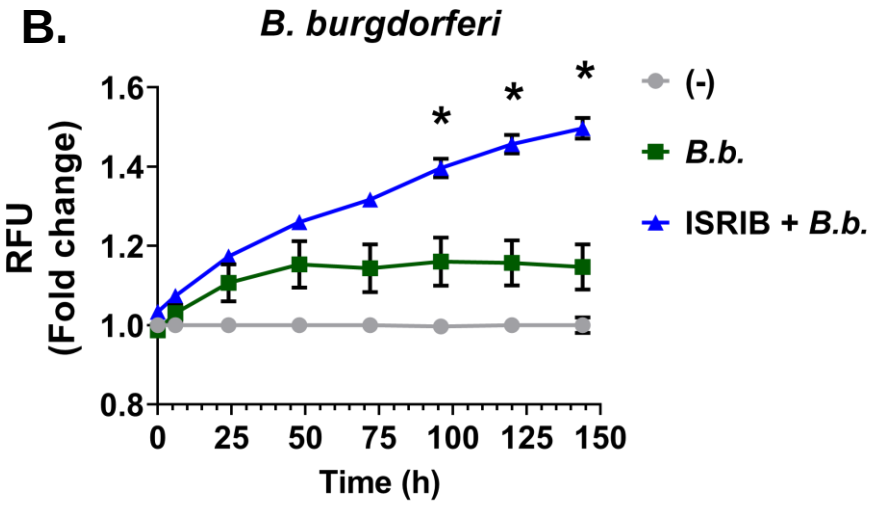

C.

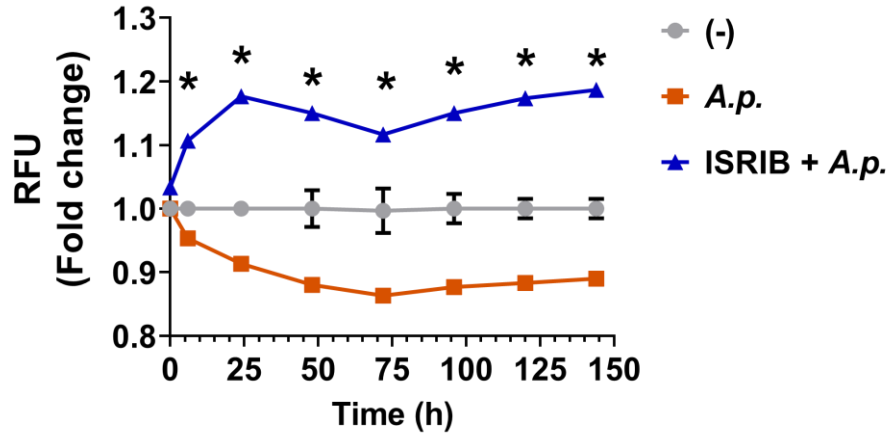

D.

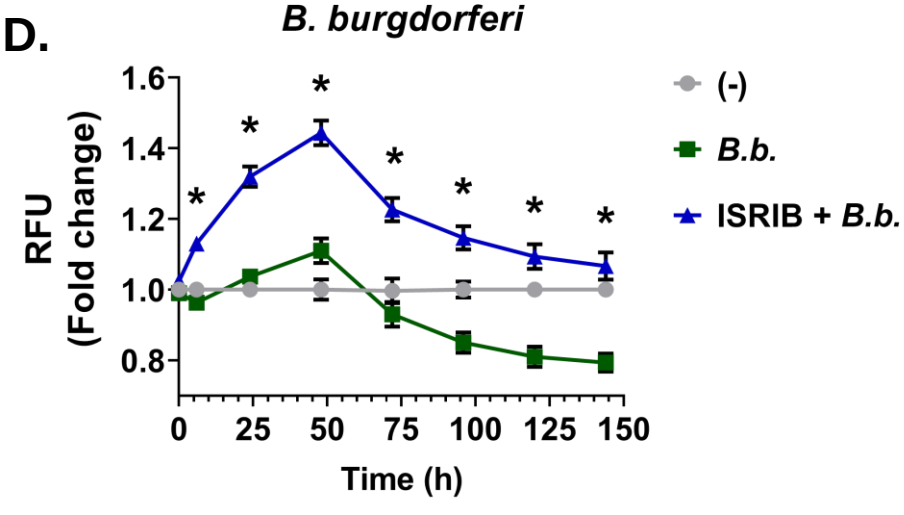

E.

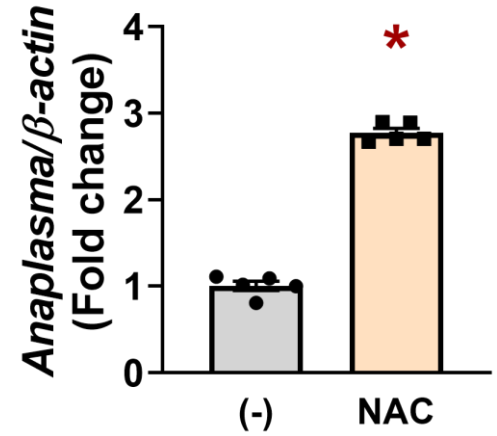

F.

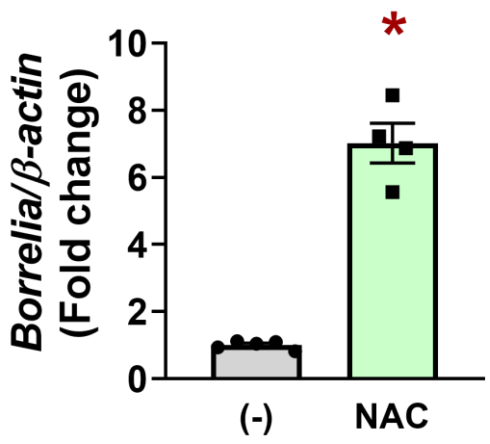

G.

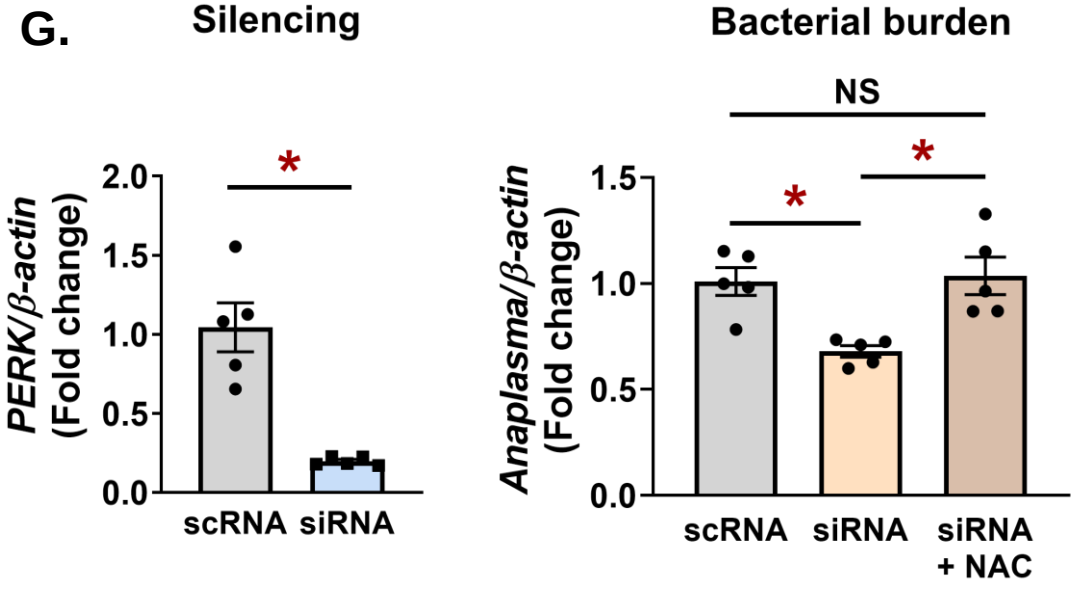

H.

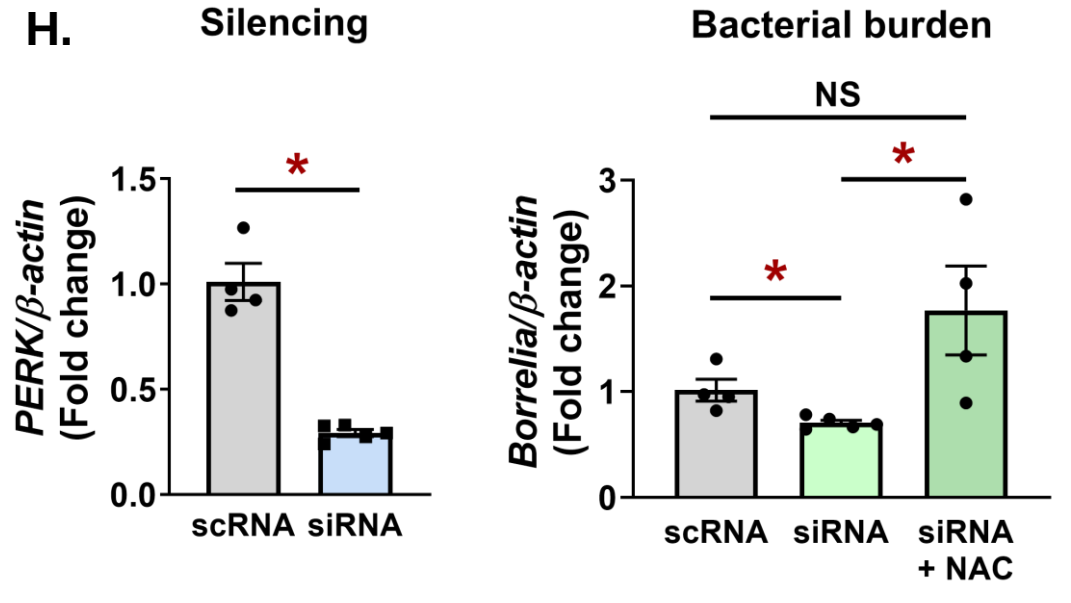

Figure 7 | The PERK-eIF2α-ATF4 axis promotes pathogen survival in ticks through an Nrf2-mediated antioxidant response.